Annu. Rev. Earth Planet. Sci. 2003. 31:469–523
doi: 10.1146/annurev.earth.31.100901.145500
First published online as a Review in Advance on January 24, 2003

RECOGNIZING MANTLE PLUMES IN THE GEOLOGICAL RECORD

Richard E. Ernst and Kenneth L. Buchan
Geological Survey of Canada, Natural Resources Canada, Ottawa, Ontario, Canada K1A 0E8; email: rernst@nrcan.gc.ca

Key Words large igneous province (LIP), FOZO, isotope, rift, dyke swarm, mantle root

■ **Abstract** Mantle plumes are recognized by domal uplift, triple junction rifting, and especially the presence of a large igneous province (LIP), dominated in the Phanerozoic by flood basalts, and in the Proterozoic by the exposed plumbing system of dykes, sills, and layered intrusions. In the Archean, greenstone belts that contain komatiites have been linked to plumes. In addition, some carbonatites and kimberlites may originate from plumes that have stalled beneath thick lithosphere. Geochemistry and isotopes can be used to test and characterize the plume origin of LIPs. Seismic tomography and geochemistry of crustal and subcrustal xenoliths in kimberlites can identify fossil plumes. More speculatively, plumes (or clusters of plumes) have been linked with variation in the isotopic composition of marine carbonates, sea-level rise, iron formations, anoxia events, extinctions, continental breakup, juvenile crust production, magnetic superchrons, and meteorite impacts. The central region of a plume is located using the focus of a radiating dyke swarm, the distribution of komatiites and picrites, etc. The outer boundary of a plume head circumscribes the main flood basalt distribution and approximately coincides with the edge of domal uplift that causes shoaling and offlap in regional sedimentation.

INTRODUCTION

Although the basic concept of mantle plumes (Figure 1) originated in the 1960s and 1970s (Wilson 1963; Morgan 1971, 1972), their role in explaining geological processes was marginalized during the plate tectonic revolution. It was recognized that a significant amount of mafic magmatism is located far from plate boundaries, but it was not clear how to incorporate such intraplate magmatism into a plate boundary paradigm. Furthermore, it became increasingly clear that the geochemistry and isotopic character of intraplate magmatism, although variable, is distinct from and requires different mantle sources (reservoirs) than mid-ocean ridge and arc basalts associated with plate boundaries (e.g., Basaltic Volcanism Study Project 1981). Questions remained regarding the distribution of the reservoirs for intraplate magmatism and whether there is a fundamental separation of

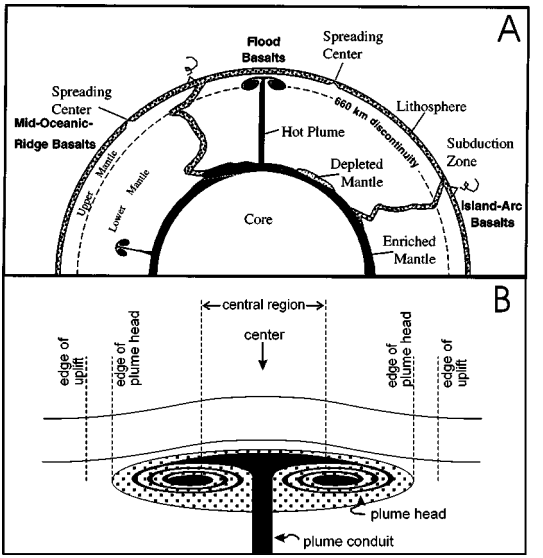

Figure 1 (*A*) A model for the relationship between mantle plumes, subduction zones, and spreading centers (after Figure 2 in Campbell 2001). Flood basalts (LIPs) and volcanic hot spot chains form above plumes, mid-ocean ridge basalts (MORBs) erupt at spreading centers, and island arc basalts (IABs) erupt above subduction zones. Rising plumes can entrain "enriched" mantle representing subducted components (EM1, EM2, and HIMU) and an ancient depleted component (FOZO). Some plumes may also originate from an intramantle boundary, and other plumes arising from the base of the mantle may stall at an intramantle boundary and spawn miniplumes (not shown) (Arndt 2000). (*B*) Schematic diagram showing the location of the geographic elements of a plume. Plume conduit is also termed the plume tail. Note that uplift is highly exaggerated.

the upper mantle reservoir for mid-ocean ridge basalts (MORBs) and lower mantle reservoirs for major intraplate magmatism (e.g., O'Nions & Tolstikhin 1996, Hofmann 1997, Kellogg et al. 1999, Albarède & van der Hilst 1999).

Mantle plumes represent buoyant material that separates from a thermal (perhaps partly compositional) boundary layer either at the base of the mantle or at the 660-km boundary and typically develops a head and tail structure as it ascends through the mantle (e.g., White & McKenzie 1989; Campbell & Griffiths 1990; Campbell 1998, 2001; Davies 1999; Schubert et al. 2001) (Figure 1). Upon reaching the base of the lithosphere, the head flattens against the lithosphere. The size of the head depends mainly on the starting depth. For plumes originating from the base of the mantle, the final diameter upon arrival at the base of the lithosphere is about 1000 km. Flattening of the plume against the lithosphere doubles the diameter to about 2000 km. For plumes starting at the 660-km boundary, the diameter upon reaching the base of the lithosphere is about 250 km, and the final diameter of the flattened plume head is about 500 km. The largest magmatic provinces are

thought to derive from plumes originating in the deep mantle, whereas small-scale Cenozoic magmatic provinces in Europe and Africa have been linked to smaller plumes rising from the 660-km boundary (e.g., Burke 1996, Wilson and Patterson 2001). However, the presence of these mini-plumes in the upper mantle can also be linked to deep-sourced plumes, that temporarily pond at a intramantle boundary (Goes et al. 1999, Wilson & Patterson 2001), or by sublithospheric channelling (Ebinger & Sleep 1998).

The general character of the model has been confirmed using seismic tomography, which has allowed direct imaging of plumes rising from both mid-mantle and deep-mantle depths (e.g., Nataf 2000, Zhao 2001, Granet et al. 1995). The return flow to the deep mantle has also been imaged in the form of subducting slabs. Some of these directly descend to the deep mantle and others flatten, perhaps only transiently, in the mid-mantle (e.g., van der Hilst et al. 1997, Kennett & van der Hilst 1998, Fukao et al. 2001) before descending into the lower mantle in global (or regional) slab avalanche events (Tackley et al. 1993; Schubert et al. 2001, p. 455; Condie 2001).

Supercomputer "experiments" (e.g., Hansen & Yuen 2002) suggest that during ascent, mantle plumes may exhibit complex behavior. They can be tilted in the "mantle wind," as are the Afar and Iceland plumes (e.g., Zhao 2001, Shen et al. 2002). They may stagnate at the 660-km boundary and spread laterally to initiate new plume upwellings in the upper mantle. For example, the Iceland plume may spread laterally to feed the European asthenospheric reservoir which in turn feeds finger-like upwellings beneath the Massif Central, Eifel, and other massif-type volcanic fields of Europe (Goes et al. 1999, Wilson & Patterson 2001). Finally, a plume may rise in multiple pulses along a single conduit (Bercovici & Mahoney 1994, Kelly & Bercovici 1997).

There is also the notion that not all plumes are created equal. In particular, a class of larger events termed "superplumes" or "superplume events" (Maruyama 1994, Ishida et al. 1999, Condie 2001) has been identified. The mid-Pacific magmatism represents the archetypal superplume event, with its associated geoid high, temporally associated eustatic sea-level rise, increased production rate of oceanic crust, and magnetic superchron (Larson 1991a,b, 1997; Maruyama 1994). However, rather than a single "superplume," this set of features may represent a broad upwelling ("superswells" e.g., McNutt 1998) through which clusters of normal-sized plumes rise (e.g., Davies 1999, Ernst & Buchan 2002). This model is supported by recent seismic mapping of mantle transition-zone thickness beneath the South Pacific Superswell, and the identification of only one deep-sourced current plume of several-hundred-kilometer diameter, rather than a "superplume" of several-thousand-kilometer diameter (Niu et al. 2002).

Individual mantle plumes are also linked to broad uplifts, rifting, continental and oceanic flood basalt provinces, giant radiating dyke swarms, and continental breakup, and have probable links to certain types of greenstone belts, kimberlites, and carbonatites (e.g., papers in Ernst & Buchan 2001a, Condie 2001). Most studies have focused on younger plumes ($\leq$250 Ma old), which are well characterized from the study of flood basalts, hot spot tracks on the ocean floor, and seismic imaging

of upwelling regions in the mantle. However, much of the record prior to 250 Ma, apart from that of greenstone belts, has received little attention mainly because of difficulties in identifying mantle plume products. This is largely due to erosion and deformation during continental collision. Examining the record of older plumes is crucial to understanding the role of plumes in geological and tectonic processes and in examining the link with plate tectonics.

This paper reviews strategies for recognizing and locating plumes, especially in the older record, and builds on recent reviews of plume characteristics (J. Geol. Soc. Jpn. 1994, Ludden et al. 1996, Burke 1996, Mahoney & Coffin 1997, Hatton 1997, Jackson 1998, Davies 1999, Pirajno 2000, Ernst & Buchan 2001a, Condie 2001, Schubert et al. 2001, Condie et al. 2002). Our discussion is grouped into the following categories (summarized in Appendix 1): (*a*) large igneous provinces; (*b*) geochemistry of plume-related basalts (including high-Mg magmas); (*c*) additional geological settings involving ophiolites, felsic magmatism, carbonatites, kimberlites, and ore deposits, that may be related to mantle plumes; (*d*) dynamic features related to plumes including uplift, rifting, and circumferential compression structures; (*e*) deep crustal and upper mantle evidence for plumes (fossil plume heads); (*f*) techniques for locating and determining the size of a plume; (*g*) review of other proposed indicators of mantle plumes such as variations in the isotopic record of marine carbonates; and (*h*) assessment of criteria for recognition of "superplume events" (plume clusters).

LARGE IGNEOUS PROVINCES (LIPs)

Links with Mantle Plumes

The most diagnostic manifestation of mantle plumes is their mafic magma production. Adiabatic decompression of the mantle plume head as it approaches and arrives at the base of the lithosphere causes partial melting, which leads to the emplacement of a LIP. The LIP consists of tholeiitic to transitional (in terms of silica versus total alkalis) flood basalts, minor alkali rocks and picrites, variable amounts of felsic rocks, an associated plumbing system of dykes, sills and layered intrusions (e.g., Figure 2*A*,*B*), and an associated mafic underplate (Baragar 1977; Fahrig 1987; Cox 1989, 1993; Campbell & Griffiths 1993; Coffin & Eldholm 1994). LIP events emplaced onto continents are termed continental flood basalts and can have volumes of up to millions of cubic kilometers (e.g., for the Siberian Traps) (Reichow et al. 2002), and those emplaced onto oceanic crust are termed oceanic plateaus or oceanic flood basalts and can have volumes up to 40-million cubic kilometers (i.e., for Ontong Java) (Coffin & Eldholm 1994, 2001; Arndt & Weis 2002). Mafic magmatism produced by deep-sourced mantle plume heads is much more voluminuous (Coffin & Eldholm 1994, 2001; Ernst & Buchan 2001b) than that produced by shallow-sourced plumes (e.g., Burke 1996, Wilson & Patterson 2001) or that associated with plume tails (e.g., Parsons et al. 1998). [Non-plume models for the origin of LIPs include the edge-convection model of King & Anderson (1998)].

Dyke swarms that radiate from the plume head center can transport magma laterally for up to 3000 km away from the plume center and can feed lava flows, sill provinces, and layered intrusions at any distance along their extent (e.g., Ernst & Buchan 1997a, 2001c). Although most LIPs occur in an intraplate setting, or along spreading ridges (e.g., Hill 1991, Coffin & Eldholm 1994), they may also arise in convergent plate tectonic regimes, i.e., a subduction zone setting (e.g., Hill 1993, Murphy et al. 1998, Wyman 1999).

Normal asthenospheric mantle is unable to melt sufficiently to produce a LIP by adiabatic decompression during plume ascent unless aided by lithospheric thinning of at least 50% (White & McKenzie 1989, Campbell 1998). However, the absence of precursor rifting in many LIP provinces lends support to an alternative model in which the addition of about 15% eclogite component, entrained in "blobs," allows more and faster melting to start at deeper levels during adiabatic rise of the plume (Cordery et al. 1997, Takahashi et al. 1998, Campbell 1998, Leitch & Davies 2001, Gibson 2002). The source of this eclogite component is considered to be descending slabs that have been recycled into rising plumes (and, as discussed later, is the probable source of some distinctive isotopic compositions).

In most cases flood volcanism begins prior to lithospheric thinning. However, a second pulse of magmatism may occur once rifting begins (Campbell 2001) owing to decompression melting caused by crustal extension (White & McKenzie 1989) and can be recognized offshore in seaward-dipping seismic reflectors (Menzies et al. 2002b). It is also possible that a second plume-head pulse can rise along an existing conduit, resulting in a second LIP (Bercovici & Mahoney 1994, Kelly & Bercovici 1997).

In the Archean, the record is more complicated. There are proper flood basalts of Archean age, such as the widespread, flat-lying Ventersdorp and Fortescue sequences of southern Africa and northwestern Australia, respectively (Eriksson et al. 2002). However, the more numerous deformed volcanic packages, termed greenstone belts, are more difficult to assess in a plume context.

Nevertheless, two classes of non-arc-related greenstone belts, the so-called mafic plains and platform assemblages (Thurston & Chivers, 1990), may be analogous to modern LIPs (e.g., Condie 2001). Based on the presence of minor komatiites, these classes of greenstone belt likely have a plume origin. Furthermore, in a few cases, notably in the Kam Group of the Slave Province, Canada, and perhaps in the Bababudan Group of Dharwar Craton, India, and in the Abitibi Belt of the Superior Province, Canada, there are sufficient data to correlate between and within greenstone belts and to demonstrate scales of basaltic magmatism similar to modern LIPs (Bleeker 2003, Ayer et al. 2002). Possible reasons why Proterozoic and Archean LIPs are typically subaqueous, in contrast to the subareal nature of Phanerozoic continental LIPs, are discussed by Arndt (1999).

High-Mg Melts

In this section, we address high-Mg magmas (komatiites and meimechites with MgO > 18% and picrites with MgO = 12%–18%) (Le Bas 2000), which are

considered diagnostic of plumes (e.g., Campbell 1998, 2001; Arndt et al. 2001; Tomlinson & Condie 2001; Condie 2001; Isley & Abbott 2002). Komatiites constitute at least 5% of the volcanic pile in about 60% of Archean greenstone belts (Figure 2 in de Wit & Ashwal 1997). Picrites are present in association with continental LIPs (Deccan, North Atlantic Igneous Province, Parana-Etendeka, Karoo-Ferrar), oceanic plateaus (e.g., Gorgona Island of the Colombian-Caribbean event), and oceanic islands (e.g., Hawaii, Iceland), and also in association with Archean komatiites (Campbell 2001, Gibson 2002).

High-Mg magmas (komatiites and picrites) represent high degrees of partial melting. Although there is some debate about their origin (e.g., Burke 1997, de Wit 1998, Smith & Lewis 1999), high-Mg magmas are generally linked with mantle plumes. They are interpreted to be generated from the hottest portion of a plume **(**Figure 1*B*), which is located above the plume conduit (e.g., Campbell et al. 1989). At pressures above 3 GPa, melting of mantle produces picrites and komatiites, and

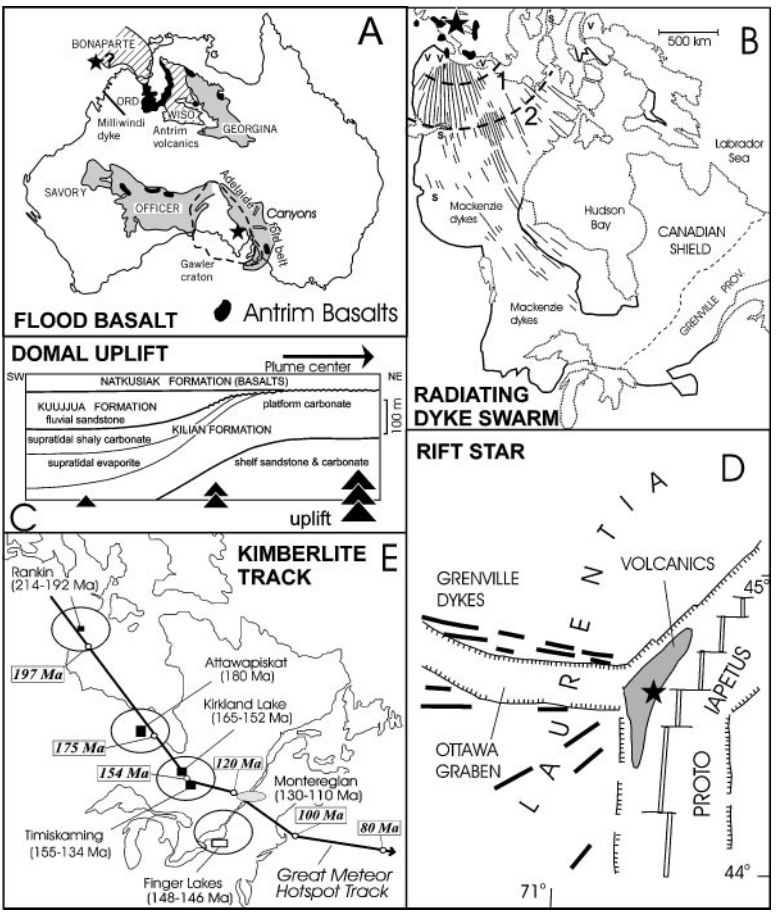

variation in normative enstatite and Al_2O_3 composition reflect plume potential temperature and depth of melting (Herzberg & O'Hara 1998). The generation of high-Mg anhydrous melts requires mantle potential temperatures that are about 200°C–300°C in excess of those of ambient upper mantle. For the modern mantle, Campbell & Griffiths (1992) have proposed that an MgO threshold of 14 wt% be used for identification of plume-related magmas, whereas an 18 wt% threshold is applied to the hotter Archean mantle. Gibson (2002) applied a similar Archean threshold but used 12 wt% for the Phanerozoic and Proterozoic.

A nonplume setting can be argued only for certain classes of high-Mg rocks. Some picrites are produced by the melting of water-rich mantle, but such arc picrites are distinguished by their low Ni, Nb, Ta, and Ti, and high K, Rb, Ba, and Pb content (Campbell 2001). Recently it has been proposed that some Archean komatiites were produced by melting wet mantle (e.g., Grove et al. 1997), which could suggest a subduction zone (i.e., nonplume) setting. It should be noted, however, that the widespread application of the wet komatiite model has been refuted by Arndt et al.

←

Figure 2 (*A*) An approximately 510-Ma LIP in Australia consisting of Antrim basalts and correlatives (Bultitude 1976, Hanley & Wingate 2000, Williams & Gostin 2000). Outcroppings are shown in black. However, the Antrim basalts and correlatives are much more extensive, underlying the Ord, Bonaparte, Wiso, Daly River, Georgina, Officer Basins (Hanley & Wingate 2000), and the Savory Basin (M. Wingate, personal communication, 2000). The grey pattern locates late Neoproterozoic–Early Paleozoic sedimentary basins, whereas the diagonal dashed pattern locates Early Paleozoic basins. In the southern Adelaide Fold Belt, there are metamorphosed mafic intrusives of the same age (Chen & Liu 1996) and deep erosional canyons (*Canyons*) that represent uplift of the Gawler craton and reflect the arrival of the Antrim plume, with the center marked by a star (Williams & Gostin 2000). A second plume (speculatively located by a star and question mark) may also be associated with the great thickness of Antrim basalts in the northern area. (*B*) Giant radiating dyke swarm converging to plume center: 1270-Ma Mackenzie swarm of Canadian Shield (after Ernst & Buchan 2001c). The curved dashed line labeled "1" marks the transition from vertical flow nearer the plume center to horizontal flow out to the end of the swarm. The curved line labeled "2" marks the approximate transition between the radiating and subparallel regions of the swarm. "s" locates sills that are probably fed from laterally flowing Mackenzie dykes, and "v" locates related volcanics. (*C*) Plume-generated domal uplift: stratigraphy of the uppermost Neoproterozoic Shaler Supergroup of the Minto Inlier, Victoria Island, northern Canada (Rainbird & Ernst 2001). Note the progressive offlap of marine facies and depositional and erosional thinning toward the plume center. (*D*) Triple junction rifting (rift star) associated with a mantle plume. Also shown is the related 590-Ma Grenville-Rideau-Adirondack radiating dyke swarm focussing near Montreal, Canada (Kumarapeli 1993). (*E*) Kimberlite age progression across North America interpreted as a hot spot track that continues through the Monteregian Intrusions and into the Atlantic as the Great Meteor hot spot track (Heaman & Kjarsgaard 2000).

(1998). One important argument relates to the high Ni content of komatiites for a given MgO value (Figure 11 in Campbell 2001).

LIP Record Through Time

Building on earlier compilations [such as Coffin & Eldholm (1994) for young LIPs, Tomlinson & Condie (2001) for Archean LIPs, and Isley & Abbott (1999) for units older than 1.5 Ga], Ernst & Buchan (2001b, 2002) compiled a LIP database and used it to assess the distribution of plume-head magmatic events in space and time back to 3.8 Ga. Three hundred and four possible LIP events were identified and divided into three classes ("well established," "probable," and "possible"). Thirty-one mafic magmatic events have been confidently related to mantle plume heads and are considered well established on the basis of the following criteria: emplacement of a large amount (areal coverage of $>100{,}000$ km^2) of magma in a short time (a few million years), the presence of a giant radiating dyke swarm, or a link to a present-day hot spot. Using other criteria, including "plume" geochemistry, the presence of high-Mg magmas (picrites and komatiites), or the presence of giant (>300-km long) linear dyke swarms, an additional 197 events are considered probable in terms of being related to plume arrival. The remaining 76 events, the majority of which are rift related, require further study to assess a plume head connection and are rated as possible.

The plume record is relatively continuous (Figure 3). A few gaps are observed, but it is not clear if these represent plume-free periods or are merely due to an incomplete database. Estimates of average plume frequency based on this record indicate an average frequency of one plume every 20 Ma since the Archean (Ernst & Buchan 2002). The apparent increase in plume frequency since 150 Ma ago is due to the presence of numerous oceanic LIPs augmenting the continental LIP record (see Figure 4 in Ernst & Buchan 2002). During ocean closure, the majority of oceanic LIPs are deformed, fragmented, and mostly subducted (Cloos 1993); therefore, oceanic LIPs are harder to recognize in the pre-150-Ma record. A late Archean increase in plume frequency from 2800 to 2700 Ma reflects either an increase in plume generation or increased preservation of LIPs, or both. The drop-off in plume flux prior to 2.8 Ga is probably mostly due to poor preservation of this older record.

GEOCHEMISTRY OF PLUME-RELATED BASALTS

In the older, more fragmentary, geological record, geochemistry provides a useful tool for assessing which magmatic events are plume related and for identifying changes in plume character with time. We begin our discussion of the geochemistry of LIPs with the chemistry of ocean island basalts (OIBs). Whereas continental and oceanic LIPs are interpreted to represent plume-head (or starting plume) events, most OIBs are considered to be the expression of plume tails. Unlike continental LIPs, OIBs are largely free of crustal contamination. They are also better studied

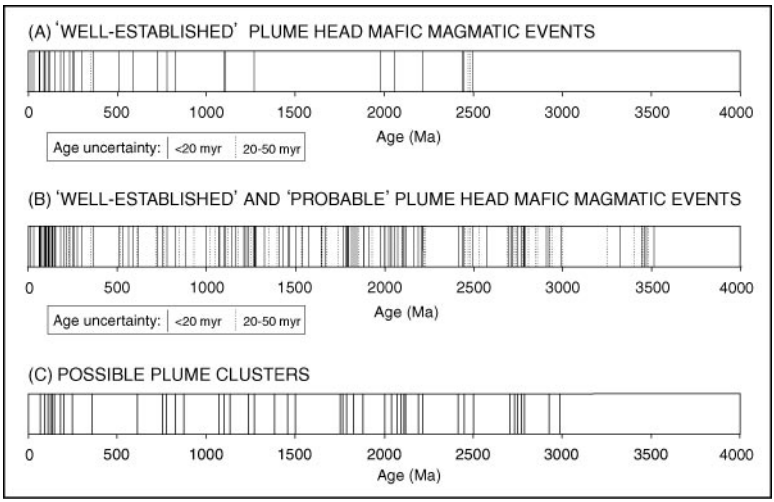

Figure 3 Spectrum of LIPs through time (after Table 1 in Ernst & Buchan 2001b). (*A*) Events rated as "well established." (*B*) Events rated as either "well established" or "probable." (*C*) Possible plume clusters defined as events of the same age occuring on more than one continental block, or on a single block if shown to be due to more than one plume (see Table 2 in Ernst & Buchan 2001b; Ernst & Buchan 2002).

than oceanic LIPs (oceanic plateaus), and they provide the clearest expression of plume sources.

Ocean Island Basalts (Plume Tail Magmas)

Based on the study of Sr, Nd, and Pb, and more recently Hf, Os, and He, isotopic systems, it is inferred that oceanic basalts are derived from five main mantle reservoirs (Table 1): DMM (depleted MORB mantle), HIMU (high μ), EM1 (enriched mantle 1), EM2 (enriched mantle 2), and FOZO (focal zone) (e.g., Zindler & Hart 1984, Hart 1988, Hart et al. 1992, Farley et al. 1992, Hauri et al. 1994, Hofmann 1997, Hilton et al. 1999, van Keken et al. 2002). DMM has low $^{87}Sr/^{86}Sr$, low $^{206}Pb/^{204}Pb$, and high $^{143}Nd/^{144}Nd$ ratios, and it is the source for MORBs around the world. This reservoir is commonly considered to be located in the upper mantle. The other four reservoirs are characteristic of the plume sources of OIBs. EM1 is characteristic of Pitcairn and Tristan Islands and has high $^{87}Sr/^{86}Sr$, low $^{206}Pb/^{204}Pb$, and low $^{143}Nd/^{144}Nd$ ratios. The other enriched component, EM2, occurs in the Society and Samoa Islands and is characterized by high $^{87}Sr/^{86}Sr$ (>EM1), moderate $^{206}Pb/^{204}Pb$, and low $^{143}Nd/^{144}Nd$ ratios. Its geochemical trends resemble continental crust. HIMU is characteristic of St. Helena, Austral-Cook Islands (Tubuai), Balleny Islands, and the Azores. HIMU represents strong enrichment of ^{206}Pb and ^{208}Pb relative to ^{204}Pb.

TABLE 1 Isotopic composition of main mantle reservoirs

Reservoir	$^{87}Sr/^{86}Sr$	$^{143}Nd/^{144}Nd$ (ε_{Nd})	$^{206}Pb/^{204}Pb$	$^{207}Pb/^{204}Pb$	$^{208}Pb/^{204}Pb$	$^{3}He/^{4}He$ (R/R_a)	$^{187}Os/^{188}Os$ (γ_{Os})	$^{176}Hf/^{177}Hf$ (ε_{Hf})
EM-1	0.70530[a,f]	0.51236 (−5.5)[a] 0.51233 (−6)[f]	17.40[a] 17.5[f]	15.47[a,f]	38.1[a] 39.0[f]	(5)[d]	~0.148 (16.5)[d]	~0.2826 (−6)[e] ~0.28262 (−5.3)[f]
EM-2	0.70780[a]	0.51258 (−1)[a]	19.00[a]	15.85[a]	39.5[a]	(6)[d]	~0.150 (18)[d]	~0.2828 (1)[e]
HIMU	0.70285[a]	0.51285 (4)[a]	21.80[a]	15.81[a]	40.8[a]	(4)[d]	~0.150 (18)[d]	0.28289 (4)[e]
DMM	0.70220[a]	0.51330 (13)[a]	18.00[a]	15.45[a]	37.5[a]	(8)[d]	~0.123 (−3)[d]	0.2833 (18.5)[e]
FOZO	0.703 to 0.704[b]	0.51280 to 0.51300 (+3 to +7)*[b]	18.50–19.50[b]	15.50–15.65[c]	38.8–39.3[c]	(35)[d]	~0.127 (0)[d]	0.28335 (20)[g]

[a]Hart (1988) with some updates after Hart et al. (1992).

[b]Hauri et al. (1994).

[c]Hart et al. (1992).

[d]estimated from Figure 6 in van Keken et al. (2002).

[e]estimated from Figures 2 and 6 in Ballentine et al. (1997).

[f]estimated from Figures 1, 3, and 5 in Eisele et al. (2002).

[g]estimated from Figure 5 in Nowell et al. (1998), and Figure 5 in Kempton et al. (2000).

*ε_{Nd} = up to +10 for picrites from the Karoo and North Atlantic Igneous Provinces (Kerr et al. 1995 and references therein) and for basalts from Iceland (Kempton et al. 2000).

ε_{Nd}, ε_{Hf}, γ_{Os} represent values normalized to CHUR (Chondritic Uniform Reservoir), whereas R/Ra represent the helium isotopic ratio relative to the ratio in atmosphere.

$\varepsilon_{Nd} = (\{[^{143}Nd/^{144}Nd]_{sample}/[^{143}Nd/^{144}Nd]_{CHUR}\}-1) \times 10^4$, where present-day $[^{143}Nd/^{144}Nd]_{CHUR} = 0.512638$.

$\gamma_{Os} = \{[^{187}Os/^{188}Os]_{sample}/[^{187}Os/^{188}Os]_{CHUR}\} \times 100$, where present-day $[^{187}Os/^{188}Os]_{CHUR} = 0.127$.

$R/Ra = [^{3}He/^{4}He]_{sample}/[^{3}He/^{4}He]_{atm}$, where present-day $[^{3}He/^{4}He]_{atm} = 1.4 \times 10^{-6}$.

$\varepsilon_{Hf} = (\{[^{176}Hf/^{177}Hf]_{sample}/[^{176}Hf/^{177}Hf]_{CHUR}\}-1) \times 10^4$, where present-day $[^{176}Hf/^{177}Hf]_{CHUR} = 0.282772$ (table 1 in Blichert-Toft et al. 2002).

An additional depleted reservoir (distinct from MORB) is suggested by the convergence of ocean island trends in Sr-Pb-Nd isotopic space (Figure 4*A*). This reservoir, FOZO, is interpreted to represent a common plume component located in the lower mantle (Hart et al. 1992, Hauri et al. 1994, Hofmann 1997, Hilton et al. 1999). The FOZO component is probably the same as PHEM (primitive helium mantle), which is seen in the He versus Sr, Nd, and Pb isotopic arrays (Farley et al. 1992, van Keken et al. 2002) and "C" (common) by extrapolating trends in MORB data (Hanan & Graham 1996, Hilton et al. 1999). This depleted component also has high $^{176}Hf/^{177}Hf$ (Kempton et al. 2000) and high $^{187}Os/^{188}Os$ isotopic ratios (Shirey & Walker 1998, van Keken et al. 2002). High $^{3}He/^{4}He$ ratios are observed at Hawaii, Iceland, Bouvet, Galapagos, Easter, Juan Fernandez, Pitcairn, Samoa, Reunion, and Heard islands, and they increase toward the FOZO component (Hofmann 1997, van Keken et al. 2002). FOZO can be distinguished from DMM by much higher $^{3}He/^{4}He$ isotope values and slightly lower $^{143}Nd/^{144}Nd$ ratios.

EM1, EM2, and HIMU components can be derived from subducted oceanic lithosphere that has been carried to depth and incorporated into rising plumes (e.g., Hofmann 1997, Condie 2001). Specifically, the HIMU component may represent the oceanic crust from which preferential loss of Pb during subduction allowed the U+Th/Pb ratio to increase with aging to produce high $^{206}Pb/^{204}Pb$ and $^{208}Pb/^{204}Pb$ ratios. EM1 has been linked to old oceanic mantle lithosphere (plus or minus sediments), or metasomatized lower mantle and recycled plume heads, and EM2 represents subducted oceanic sediments, essentially reflecting a continental crust signature (e.g., Condie 2001). In short, the conventional view is that EM2 represents a continental crust component, EM1 represents mantle lithosphere, and HIMU represents oceanic crust. It is possible that recycled subducted slabs contribute to high $^{3}He/^{4}He$ and $^{187}Os/^{188}Os$ values in plumes because of ^{4}He loss during subduction and because ^{187}Re, the parent for ^{187}Os, is retained in the mantle during partial melting to produce the oceanic crust (Shirey & Walker 1998). In particular, $^{187}Os/^{188}Os$ values show a remarkable convergence toward FOZO when plotted against $^{206}Pb/^{204}Pb$ values; this is interpreted by van Keken et al. (2002) as the "smoking gun" for slab recycling. It has also been argued that high $^{3}He/^{4}He$ and $^{187}Os/^{188}Os$ values are primordial. In addition, high values of $^{186}Os/^{188}Os$ appear to reflect leakage from the core because ^{186}Os is the daughter of ^{190}Pt (Brandon et al. 1999).

An alternative model by Anderson and others (Anderson 1995, King & Anderson 1998) suggests that the enriched reservoirs are not in the deep mantle but are located in the upper mantle along with DMM, the MORB source.

The age of formation of these isotopic reservoirs is important in interpreting the isotopic data from older LIPs. The HIMU, EM1, and EM2 reservoirs of the OIB source became significant in the Paleoproterozoic and probably date from that time. This is reasonable in terms of models in which subducted slabs accumulate in the deep mantle (Campbell 1998). However, FOZO may represent a still-older depleted component that developed during the Archean (Campbell 1998). Hf isotopic values also suggest an Archean age for the depleted component (Kempton et al. 2000).

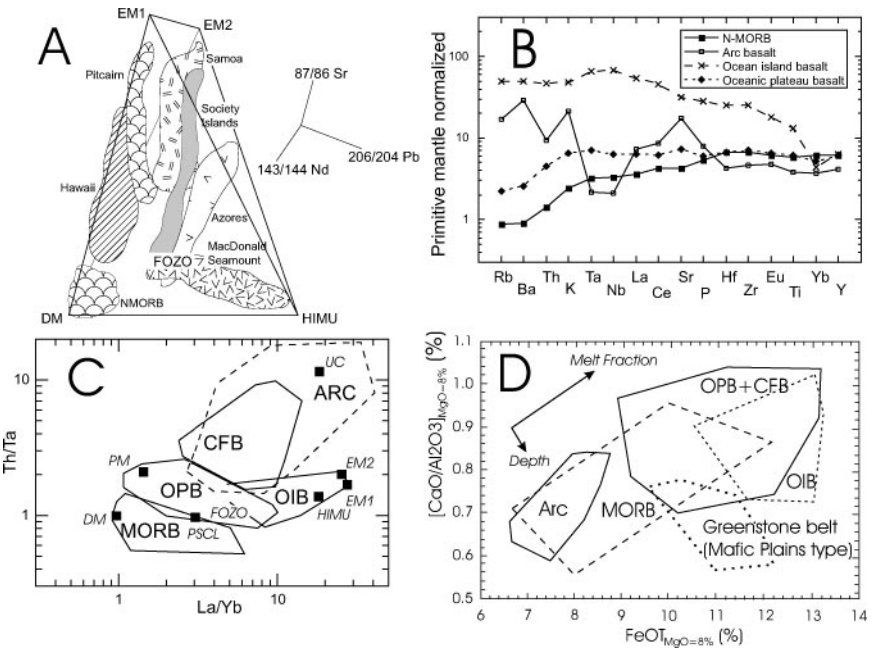

Figure 4 Geochemical diagrams. (*A*) Mantle tetrahedron (from Condie 2001, after Hart et al. 1992). Geochemical reservoirs in mantle and the identification of the common depleted deep mantle "plume" component, FOZO (focal zone), based on the distribution of oceanic basalts in Sr-Nd-Pb isotopic space (after Hart et al. 1992). The corners of the tetrahedron are the principle mantle reservoirs. (*B*) Spider diagrams for basalts from various tectonic settings (Figure 5.1 in Condie 2001, Figure 1 in Tomlinson & Condie 2001). (*C*) "Condie" diagram Th/Ta versus La/Yb diagram showing fields for main basalt types and locations of reservoirs. FOZO is only approximately located. Diagram after Figure 2 in Tomlinson & Condie (2001), with additions from Figure 5.11 in Condie (2001). (*D*) $[CaO/Al_2O_3]_{\text{for MgO} = 8\text{wt\%}}$ versus $[FeOT]_{\text{for MgO} = 8\text{wt\%}}$ (where FeOT represents combined FeO and Fe_2O_3 expresses FeO), after Figures 7.3 and 4.17 in Condie (2001). Accreted oceanic plateaus (Figure 6.6 in Condie 2001) plot similarly to the Archean greenstone belts of the mafic plains association. With increasing depth of origin (and higher mantle potential temperature), FeOT increases and CaO/Al_2O_3 decreases, and with increasing melt fraction at a given pressure, both FeOT and CaO/Al_2O_3 increase (Condie 2001, p. 140; Lassiter & DePaolo 1997). Basalt types are: MORB (mid-ocean ridge basalt), OIB (ocean island basalt), CFB (continental flood basalt), OPB (oceanic plateau basalt), ARC (subduction zone basalt). Principle mantle reservoirs are: EM1 (enriched mantle 1), EM2 (enriched mantle 2), HIMU ('High μ', $\mu = {}^{238}U/{}^{204}Pb$]), DMM (depleted MORB mantle) and FOZO. Additional components are PM (primitive mantle), PSCL (post-Archean subcontinental lithosphere), and UCC (upper continental crust).

The data from carbonatites are also relevant because they show the same mantle reservoir ages (Bell & Tilton 2001, 2002). Sr, Nd, Pb, and Hf isotopic data from carbonatites (Bell & Tilton 2002) require persistence of the depleted (FOZO) reservoir since the late Archean (for Pb and Sr isotopes), and since at least 3 Ga for Nd and Hf isotopes. Furthermore, as noted by Bell & Tilton (2001, 2002), carbonatites can have primordial values of $^{129}Xe/^{130}Xe$ and $^{40}Ar/^{36}Ar$ (Sasada et al. 1997), which supports the idea of a long-lived isolated reservoir for FOZO. Hf isotopic studies of carbonatites and kimberlites also indicate that enriched plume sources (HIMU and/or EM1) have existed since 3 Ga (Bizzarro et al. 2002).

LIPs (Plume-Head Magmas)

On Nd-Sr isotopic diagrams, oceanic plateaus plot (similar to OIBs) between depleted mantle and chondrite, in the vicinity of HIMU and FOZO. Some are clearly influenced by EM1 and EM2. Continental flood basalts typically plot in the field of negative ε_{Nd} and enriched $^{87}Sr/^{86}Sr$ owing to contamination by continental crust. It is possible to use Os isotopes to distinguish crustal contamination from contamination owing to subcontinental lithosphere (e.g., Figure 5.16 in Condie 2001). The $^{3}He/^{4}He$ ratio is also very diagnostic. MORB values are constant at 8 (R/R_A, the He isotopic ratio in the sample divided by the ratio in air). In contrast, much higher values are found in OIBs (except for HIMU types), continental flood basalts (e.g., Hilton et al. 1999, Basu et al. 1995; see summary in Figure 1 in van Keken et al. 2002), and in some greenstone belts of Archean age (e.g., Gibson 2002).

It should be noted that using the radiogenic isotopes to study older rocks requires correction for in situ decay of parent isotopes. Linking older LIPs to the isotopic reservoirs identified in the younger record is facilitated using epsilon, gamma nomenclature (ε_{Nd}, γ_{Os}, ε_{Hf}) for isotopic compositions (Table 1). This normalizes the data to represent deviations from chondritic composition to account for its isotopic evolution with age.

Incompatible Elements

Incompatible-element ratios may represent another tool for characterizing mantle sources because the ratios of incompatible elements in mantle source areas are preserved, particularly for high degrees of partial melting.

Starting in the 1970s, a number of diagrams, mainly based on incompatible elements, were devised to distinguish intra- (within-) plate magmatism from MORB and arc basalts and to monitor the effects of alteration and crustal contamination (e.g., Pearce & Cann 1973, Winchester & Floyd 1977, Shervais 1982, Thompson et al. 1983, Meschede 1986, Kerrich & Wyman 1997). Normalized multi-element plots (or spidergrams) show that the OIB pattern is characterized by a light rare earth element (LREE) enriched pattern with a small positive Ta-Nb anomaly (Figure 4*B*). In contrast, the MORB pattern is characterized by LREE depletion, which represents a prior melting event(s). Arc basalts are

distinguished by relative Nb-Ta depletion and Pb enrichment, characteristics acquired as the result of fluid processes during subduction (e.g., Hofmann 1997, Condie 2001).

However, the incompatible element signature of plume-head melts can be more complicated and less diagnostic because of the potential entrainment of host mantle during plume ascent (Campbell & Griffiths 1990), particularly material from the lower mantle (Campbell 1998), and also because of contamination by subcontinental lithosphere and continental crust. Some continental flood basalts (CFBs) have spidergram patterns (Figure 4*B*) that resemble OIBs. Others have depleted compositions that resemble MORB but are of lower mantle origin (e.g., Kerr et al. 1995) probably reflecting the presence of the FOZO component. However, in many cases, the data are clearly contaminated by continental crust (and continental lithosphere) and can exhibit negative Nb and Ta anomalies resembling arc rocks (Hofmann 1997). Oceanic plateaus (and Archean greenstone belts of the mafic plains assemblage) commonly have incompatible element patterns resembling MORB in the depletion of highly incompatible elements (e.g., Arndt & Weis 2002, Condie 2001). (In a recent review, Bleeker (2002) concluded that many Archean greenstone belts, including some of mafic plains type, are autochthonous (to parautochthonous) overlying felsic basement and, therefore, their origin as oceanic plateaus is suspect.) As summarized by Hofmann (1997), the ratios of Ba/Rb, K/U (except in HIMU magmas), Nb/Ta, Zr/Hf, Y/Ho, Ti/Sm, Sn/Sm, and P/Nd are constant for oceanic basalts (both OIB and MORB) and continental crust. Nb/Ta, Zr/Hf, and Y/Ho ratios also match the chondritic ratios of primitive mantle (Hofmann 1997). Element ratios that can be used to monitor the contribution of continental crust are Nb/U, Ta/U, and Ce/Pb (see Appendix 1). These ratios are similar in MORB and OIB, but much lower values are found in continental crust and island arc volcanics (and primitive mantle) (Hofmann 1997). For example, the Nb/U ratio for OIB and MORB is about 47, whereas that for chondrites and primitive mantle is about 32 and that for continental crust is about 10. The Nb/U versus Nb/Th or Nb/U versus Nb diagrams are useful for distinguishing OIB and MORB sources and assessing the prior extraction of continental and oceanic crust (Campbell 1998, 2002). Similarly, mantle reservoir sources can be distinguished on the Th/Ta versus La/Yb "Condie" diagram (Figure 4*C*) (Condie 1997, 2001). The ratios Ba/La, Rb/La, Th/U, and Th/La are generally greater than (or equal to) the respective source areas (Hofmann 1997). Thus, if a source has had a prior melt extraction, these ratios will be lower than primitive mantle values. However, ratios involving Ba, K, Rb, and U are less useful in assessing older rocks because of the mobility of these elements during alteration events.

Another important pair of ratios are La/Sm and Sm/Yb, which represent the slopes of the light to middle rare earths and middle to heavy rare earths, respectively. Partial melting of either garnet or spinel peridotite will preferentially enrich the basalts in lighter REEs (rare earth elements). But if significant partial melting occurred at a sufficient depth for garnet to remain in the source area, then the middle

to heavy REE ratio (i.e., Sm/Yb) in the melt will increase (e.g., Lassiter & DePaolo 1997). This is more significant for continental flood basalts, which are typically generated at a greater depth (under a lithospheric "lid") than oceanic flood basalts. Further discussion of the effect of lithospheric lids is found in Saunders et al. (1997) and Lassiter & DePaolo (1997). The degree of melting is also important; REE patterns flatten under higher degrees of partial melting (more characteristic of oceanic flood basalts than continental flood basalts). Subsequent low-pressure fractional crystallization of basalts will change REE slopes only modestly. Therefore, after filtering the data for the effects of continental contamination (e.g., Lassiter & DePaolo 1997), the La/Sm versus Sm/Yb diagram allows monitoring of the depth of mantle source areas (i.e., the effect of a lithospheric lid) and also the degree of partial melting. A method to invert REE data to obtain the melt fraction as a function of depth is detailed by White & McKenzie (1995).

Compatible Elements

Various elements that are compatible during mantle melting may also be diagnostic of ancient mantle plumes. For example, the CaO/Al_2O_3 and iron contents of basaltic magma are sensitive to depth and degree of partial melting (Lassiter & DePaolo 1997). They show (Figure 4*D*) (Figures 4–17 in Condie 2001) that plume-head and plume-tail magmatism exhibit a greater degree of partial melting and greater depth of partial melting than arc basalts and most MORB. Comparison of these values for rocks of the mafic plains association (of Archean greenstone belts) indicate similarities with oceanic plateaus, but perhaps even deeper sources (Condie 2001, p. 199).

High nickel contents for a given whole-rock MgO are another tool (Arndt 1991, Campbell 2001) for recognizing plume involvement. Also useful is the chromium content of olivine in equilibrium with chromite (Campbell 2001). This value is strongly temperature dependent and weakly dependent on oxygen fugacity; plume-derived magmas can have >800 ppm Cr in olivine, whereas island arc magmas have <800 ppm Cr in olivine.

High-Mg Rocks

Although high-Mg rocks (komatiites, meimechites, and picrites) are volumetrically less significant than basalts, they are important in interpreting the LIP record because their high degree of partial melting better preserves the mantle ratios of less incompatible elements such as Pr, Nd, and Sm (e.g., Campbell 2002). High-Mg rock types that are present in Phanerozoic LIPs include picrites, ferropicrites, and more rarely komatiites. Types distinguished in the Archean are Al-depleted and Al-undepleted komatiites (Xie et al. 1993, Xie & Kerrich 1994, Fan & Kerrich 1997) and ferro-komatiites/picrites (Gibson 2002). The decrease in MgO contents of melts from the Archean to the present is interpreted to indicate both a decrease in depth of adiabatic decompression melting of mantle plumes and a decrease in mantle potential temperature (e.g., Gibson 2002).

Two types of Archean komatiites can be characterized geochemically in terms of origin (Xie et al. 1993, Xie & Kerrich 1994, Fan & Kerrich 1997, Kerrich & Wyman 1997, Condie 2001, Sproule et al. 2002). The first type, Al-undepleted komatiites, have near chondritic Al_2O_3/TiO_2 and Ti/Zr ratios and relatively flat, heavy REE patterns. Such komatiites have flat or depleted incompatible element abundances. The second type, Al-depleted komatiites, have low Al_2O_3/TiO_2 and Ti/Zr ratios with fractionated REE patterns. They typically show relative enrichment in incompatible elements (Arndt 1994; Condie 2001, p. 203). Some Al-depleted komatiites exhibit high La/Yb(n) (light REE enriched, n = ratio normalized to primitive mantle) slopes, along with negative Zr and Hf anomalies, consistent with majorite garnet remaining in the restite during partial melting at depths between 300 and 600 km (Xie et al. 1993; Agee 1993; Condie 2001, p. 202). The signature of perovskite can also be important in demonstrating a plume origin because Mg-perovskite becomes the major liquidus phase at 24 GPa. Melting of perovskite may be recognized by positive Nb-Ta and Zr-Hf anomalies and La/Yb(n) <1; residual perovskite in the source area will have the opposite signature. Negative Nb-Ta anomaly along with La/Yb(n) >1 but no Zr-Hf anomaly reflects crustal contamination. To summarize, Nb/Nb^*, Ta/Ta^*, Zr/Zr^*, and Hf/Hf^* ratios versus La/Yb(n) diagrams (where starred values are interpolated values from adjacent elements on primitive normalized multi-element plots) are useful for distinguishing in komatiites the effects of majorite garnet fractionation, Mg-perovksite in the source area, and crustal contamination (Figure 7.8 in Condie 2001).

The third greenstone group, the ferro-picrites and ferro-komatiites, are analgous to the ferro-picrites that are present in some Phanerozoic flood basalts (Gibson 2002). They are observed as thin layers at the base of LIP sequences of Archean age (e.g., the Onverwacht Group, South Africa, and in the Superior Province, Canada) and of Phanerozoic age (Siberian traps, Paraná-Etendeka, and North Atlantic Igneous Province) (Gibson 2002). These ferropicrites are interpreted to represent melting of streaks of eclogite, which represent paleosubduction zone material entrained in the plume head.

Geochemistry Summary

Uncontaminated plume-generated basaltic rocks should have flat REE patterns or LREE-enriched patterns and lack negative Nb, Ta, and Ti anomalies. The presence of high-MgO magmas (picrites and komatiites) is considered diagnostic of plumes. Plots such as CaO/Al_2O_3 versus Fe can be used to monitor depth and degree of melting in a plume (Figure 4*D*). Contamination by continental crust or lithosphere can impart subduction-type signatures and lead to the misidentification of basalts as arc related (Campbell 1998). High $^3He/^4He$ ratios >10 R/R_A and high Os isotopic ratios are probably diagnostic as they imply either a primordial deep source or recycled oceanic crust. Furthermore, osmium isotopes can be used to distinguish between crustal and lithospheric contamination.

ADDITIONAL GEOLOGICAL "SETTINGS" THAT MAY BE RELATED TO MANTLE PLUMES

Some other geological "settings" have been proposed to be associated with mantle plumes. These include some classes of ophiolites, felsic magmatism, kimberlites, carbonatites, and ore deposits.

Ophiolites

Oceanic LIPs are important in the young record and probably in the Archean. In the present ocean basins (back to 150 Ma) there are at least a dozen oceanic plateaus (and ocean-basin flood basalts) that are thought to be derived from plumes (e.g., Coffin & Eldholm 2001, Ernst & Buchan 2001b, Arndt & Weis 2002). In the Archean, there are at least 14 greenstone belts that are interpreted to represent oceanic plateaus (Tomlinson & Condie 2001, Arndt et al. 2001, see also listing in Ernst & Buchan 2001b). [However, Bleeker (2002) urges caution in the identification of Archean oceanic plateaus because of indications that some proposed examples were actually emplaced onto continental crust.] The intervening Proterozoic and Phanerozoic record is thought to be largely devoid of oceanic LIPs, which are efficiently removed during the subduction/collision process (Cloos 1993). One notable exception is the 2.1- and 2.2-Ga Birimian magmatism of western Africa (Abouchami et al. 1991, event 187 in Ernst & Buchan 2001). However, it is increasingly being recognized that, although ophiolites have a variety of origins (Dilek et al. 2000), accreted and underthrust terranes of ophiolitic character may represent part of this lost oceanic LIP record (Coffin & Eldholm 2001, Moores 2002).

In detail, comparison of ophiolites with modern oceanic environments suggests four end-member origins: "fast-spreading ridges (complete ophiolite sequence), slow-spreading ridges (incomplete sequence with serpentinite overlain by extrusives and/or sediments), intra-arc environments (island arc sequences intruded by mafic-silicic dyikes and intrusive bodies), and hot spot (plume) sequences consisting of thick sequences of mafic-ultramafic intrusive-extrusive rocks, but lacking the tectonite mantle characteristics of most Phanerozoic ophiolite complexes" (Moores 2002). Such "plume" ophiolites should preserve a deep-mantle signature in support of a plume origin. For instance, the Luobusa podiform chromites within the Yarlungzangbu ophiolite of southern Tibet (Bai et al. 2000) contain high-pressure mineral phases, which suggests a deep-mantle origin (Bai et al. 2002), as well as W and Os metallic nuggets with W and Os isotopic ratios consistent with a core origin (Hirata & Yang 2002).

Felsic Magmatism

Silicic volcanic rocks are an important component of LIPs, some of which are linked to plumes and some of which have plate boundary origins. Nearly all CFBs and volcanic-rifted margins have associated felsic volcanics with eruptive volumes

$>10^4$ km^3 (Bryan et al. 2002). The felsic component usually occurs as large-volume ignimbrites associated with caldera complexes and has compositions that are predominately dacite-rhyolite near the hydrous granite minimum. It originates because the heat flux from the basaltic magma results in partial melting of the lower crust unless that crust has previously been melted and is already refractory. In some cases, the isotopic character of the silicic LIP matches that of the mafic LIP, suggesting remelting of the mafic underplate. In general, the distribution of associated granitoids will be controlled by the hottest magmas and the most fusable crust. The former may suggest an association with the region above the plume conduit (Figure 1*B*). The latter suggests that a key to generating large volumes of silicic magma preserved in silicic LIPs is the prior formation of hydrous, highly fusible lower crust (Bryan et al. 2002). Specifically, partial melting (∼20%–25%) of this fusible crust will generate melts of intermediate to silicic composition. Therefore, according to Bryan et al. (2002), an earlier subduction event is crucial to the development of a hydrous, fusible lower crust (i.e., mafic to intermediate, transitional to a high-K calc-alkaline, meta-igneous source).

Significant silicic LIPs include the Chon Aike component in Patagonia and southern South America of the 183-Ma Karoo-Ferrar plume event (Pankhurst et al. 1998, Bryan et al. 2002), and the Whitsunday volcanic province (mainly 120–105 Ma) of eastern Australia, which is associated with continental breakup (Bryan et al. 2002). Other silicic LIPs in an intraplate setting include the Paleozoic Lachlan belt of Australia (Hill et al. 1992, King et al. 1997), the 745-Ma Malani rhyolites of India (Bhushan 2000, Torsvik et al. 2001), and the 1592-Ma Gawler Province felsic volcanics of southern Australia (event 129 in Ernst & Buchan 2001b). Although it should again be emphasized that not all felsic LIPs can be linked to a plume. For instance, the Tertiary-aged Sierra Madre Occidental silicic LIP of Mexico represents the largest silicic LIP at 296,000 km^3 (Table 1 in Pankhurst et al. 1998), but it has a back-arc setting (Bryan et al. 2002). The previous examples consist dominantly of volcanic rocks (mainly ignimbrites), but in areas of deeper erosion, silicic LIPs should consist of felsic (granitoid) intrusions and felsic dyke swarms.

Although felsic intrusions are most characteristically generated above subduction zones, some suites that are coeval with nearby mafic LIPs may represent the silicic intrusive component of that LIP. Examples include the widespread 250-Ma granites linked with the Siberian Traps (Dobretsov & Vernikovsky 2001), the 825-Ma intrusions associated with the South China Plume event (Li et al. 1999), and the granitoids associated with the plume-generated greenstone belts of the Yilgarn Province (Campbell & Hill 1988).

There may be potential for distinguishing plume-related anorogenic A-type granitoids from arc-related granitoids using various trace element–descriminant diagrams (e.g., Barbarin 1999). Examples include Rb versus Y+Nb (e.g., Pearce et al. 1984, Förster et al. 1997), Nb versus Y (Pearce et al. 1984), Zr versus Ga/Al (Whalen et al. 1987), and Y versus Nb versus Ga*3 (Eby 1992). A detailed geochemical review shows that oceanic intraplate and continental intraplate groups

(associated with alkaline ring complexes, active rifts, continental flood basalts, and attenuated continental crust) all plot convincingly in the WPG (within-plate granites) field in the Rb-Y+Nb diagram (Förster et al. 1997). For example, the felsic intrusions associated with the Siberian Traps in the western Taymyr region are metaluminuous and contain elevated Rb, Sr, Ba, and Nb. They can be characterized as A-type granitoids that formed in an intraplate setting (Dobretsov & Vernikovsky 2001).

One final observation relates to the migration of felsic caldera complexes with time, such as those associated with the Snake River Plain (e.g., Parson et al. 1998) of the Yellowstone plume event and those in Ethiopia-Yemen associated with the Afar plume event (Ukstins et al. cited in Bryan et al. 2002). In the Snake River Plain, the calderas likely mark the >500-km track of the tail of the Yellowstone plume between 17 Ma and the present [although an alternative entirely upper mantle origin for the Yellowstone hotspot is suggested by Christiansen et al. (2002)]. The linear distributions of calderas may, in some cases, mark the track of a plume trail.

Carbonatites and Kimberlites

Carbonatites and kimberlites are generated from low-volume melts that, in some cases, may be linked with mantle plumes. Bell (2001, 2002) has proposed a plume model to explain the close spatial relationships of volatile-rich rocks, such as carbonatites, kimberlites, and lamprophyres. It involves a low-degree partial melting in the more volatile-rich cooler parts of the plume head.

CARBONATITES Although diverse origins have been proposed for carbonate-rich magmas (e.g., Bailey 1993, Wooley 1998), there is increasing evidence that many carbonatites are linked with mantle plumes (Bell 2001), including both plume heads and plume tails. In particular, some carbonatites are associated, both spatially and temporally, with flood basalts (plume head magmas), including the Deccan, Paraná-Etendeka, Siberian, and Keweenawan events (Bell 2001). Other carbonatites, such as those of the Cape Verde and the Canary Islands, are associated with plume tails. Still others may be plume related on the basis of isotopic evidence for plume involvement. These include the carbonatite-nephelinite magmatism of East Africa and the carbonatite-pyroxenite-melilitolite associations of the Kola Peninsula, Russia (Bell & Tilton 2001, Bell 2001). Geochemical evidence for plume involvement with carbonatites includes (*a*) the similarity of Nd, Pb, Sr, and He isotopic data between most young carbonatites and OIBs and (*b*) the primitive noble-gas signatures (Ar, Ne, Xe) from some carbonatites. For example, Pb, Sr, and Nd isotopic data from carbonatites in the East African Rift exhibit linear trends between HIMU and EM1 components, whereas a second group of so-called Reference Carbonatites involve FOZO (Bell & Tilton 2001). The model favored by Bell (2001) is one in which carbonated magmas result from the low-degree melting of volatile-rich plume material trapped below thick lithosphere.

KIMBERLITES Kimberlites and the related clan of lamproite rocks represent ultramafic volatile-rich magmas that were rapidly and explosively emplaced (e.g., Helmstaedt 1993; Mitchell 1995; Haggerty 1999a,b; Schissel & Smail 2001). They are mainly found in Archean cratons and Paleoproterozoic mobile belts surrounding cratons (Haggerty 1999a). Kimberlites can be interpreted to represent a deep-sourced equivalent of basalts that are trapped beneath a lithospheric root (Campbell 2001), and can be classified into Group I (basaltic) and Group II (micaceous) types (e.g., Schissel & Smail 2001), the latter termed orangeites by Mitchell (1995). Diamonds are picked up and transported during magma ascent as xenocrysts. Inclusions within diamonds indicate that the host kimberlite (and lamproite) magmas originated at depths below 180 km and perhaps from the core-mantle boundary. Some diamonds contain inclusions of majoritic garnet (and its exsolution products) and Na pyroxene-enstatite solid solutions, which are evidence for an origin at transition zone depths (410–660 km). Other inclusions in diamonds are indicative of a lower mantle origin. Finally, some diamonds contain Fe, FeC, and SiC inclusions that may originate in Earth's core (Haggerty 1999a,b). The deep origin of these constituents is most compatible with a mantle plume origin (Haggerty 1999b). However, nonplume origins for kimberlites have also been proposed (e.g., Helmstaedt 1993, Mitchell 1995).

On a global scale, kimberlite magmatism seems to be episodic, with seven major events catalogued between 1 Ga and 50 Ma (Haggerty 1999b). Events occurred at about ~1 Ga (Africa, Brazil, Australia, Siberia, India, and Greenland), ~450 to 500 Ma (Archangel on the White Sea, China, Canada, South Africa, and Zimbabwe), 370 and 410 Ma (Siberia and United States), ~200 Ma (Botswana, Canada, Swaziland, and Tanzania), 80 to 120 Ma (south, central, and west Africa; Brazil; Canada; India; Siberia; and the United States), and ~50 Ma (Canada and Tanzania), with minor fields in Ellendale in northwest Australia at 22 Ma (Haggerty 1994). However, the age distribution of kimberlites needs to be reevaluated in light of the increasing database of high-precision U-Pb perovskite ages (e.g., Heaman & Kjarsgaard 2000). The episodicity and the time correlation with the mid-Cretaceous superplume event and with magnetic superchrons (Johnson et al. 1995) suggested to Haggerty (1994) that kimberlite formation was linked to a "superplume cycle" and associated CFB events.

However, there is also evidence for an age progression along "tracks" of kimberlites requiring a plume-tail origin. In particular, precise dating of perovskite from kimberlites identified an age progression over 2000 km in length in North America (Heaman & Kjarsgaard 2000). This provides a link with the Great Meteor hot spot track, which is considered a plume tail (Figure 2*E*). There are also kimberlite clusters in southern Africa but no age progression has been recognized, and a correlation with Discovery, Tristan, Shona, and Bouvet hot spots is not clear. However, there is a correspondence between the location of 120–110-Ma Group II kimberlites with the back-tracked positions of the Discovery and possibly the Tristan hot spots (Schissel & Smail 2001).

Ore Deposits

Several ore deposit types have a strong link with mantle plumes (e.g., Pirajno 2000, Schissel & Smail 2001). As discussed above, the primary occurrence for diamonds is in kimberlites, which have been clearly linked with mantle plumes. Some magmatic sulphide and oxide ores can be related to CFB provinces, including the Noril'sk-Talnakh PGE (platinum group element) ores of the Siberian Traps and the Duluth Complex Cu-Ni ores of the Mid-Continent Rift (Keweenawan) system. There are also the great PGE, Cu, and Ni ore deposits associated with large layered mafic-ultramafic intrusions, such as the Great Dyke of Zimbabwe and the Bushveld complex, and the Ni-sulfide ores that are associated with komatiites (e.g., Kambalda, Yilgarn Province) and picrites (e.g., Pechanga, Russia). Finally, some giant hydrothermal ore deposits can be linked to plumes (Pirajno 2000). These include the giant Kidd Creek volcanogenic massive sulfide deposit dating from 2700 Ma (Timmins, Canada) (Bleeker et al. 1999, Wyman et al. 1999) and the 1600 Ma giant Olympic Dam deposit (southern Australia) associated with the Gawler craton felsic LIP (Pirajno 2000).

DYNAMIC FEATURES RELATED TO PLUMES

Domal Uplift

There is no known process on Earth, other than the arrival of mantle plumes at the base of the lithosphere, that can form domes 1000 km or more in diameter and 1–2-km high (Figure 1*B*) within a time span of several million years (Şengör 2001). As discussed earlier, the dimensions of the uplift depend on the size of the plume head and thus on the depth at which the plume originates. For a plume rising from the deep mantle, the lithosphere is uplifted by one or two kilometers over an area comparable to the size of the flattened plume head, i.e., about 2000–2500-km diameter (e.g., White & McKenzie 1989, Campbell & Griffiths 1990, Hill 1991, Rainbird & Ernst 2001). For plumes rising from a shallower level, such as the 660-km discontinuity, the plume-head size (after flattening against the lithosphere), and hence the uplift area, should be smaller, about 500 km in diameter (Campbell 2001). Uplift is a combination of initial purely dynamical support, followed by squeezing (dynamical erosion) of the ductile lithosphere and thermal expansion caused by longer-term heating of the mechanical lithosphere (e.g., Monnereau et al. 1993, Şengör 2001). Continued plume-tail flux after the plume-head event is represented by a hot spot track. The plume tail also produces domal uplift that can be elongated by plate movement relative to the hot spot (Sleep 1990).

In the young (Cenozoic/Mesozoic) record, plume-generated uplift produces radiating drainage patterns except where modified by rifting of the domal uplift. Examples cited by Cox (1989) include the 65-Ma Deccan event of India, the

62-Ma North Atlantic Igneous Province, the 133-Ma Paraná-Etendeka event of South America and southwestern Africa, and the 183-Ma Karoo-Ferrar event of Africa and Antarctica. In the older record, radial drainage patterns are preserved as radiating paleocurrent patterns. Uplift will also lead to shoaling and thinning of sedimentary packages in the center of uplift. The region of thinned strata expands outward with continuing uplift and erosion (Figure 2*C*). Unconformities will be formed with younger overlying units that postdate the uplift. A sedimentary record of plume-generated uplift has been recognized for magmatic events ranging from 2770 to 60 Ma (Rainbird & Ernst 2001 and references therein). They include the 2770-Ma Fortescue sequence of northwestern Australia; the ca. 1800-Ma activity associated with the Richmond Gulf rift and uplift of eastern Hudson Bay (Canada); the 723-Ma Franklin dyke swarm event of northern Canada; the 615–550-Ma magmatism of the Iapetus margin of eastern Canada; the 510-Ma Antrim flood basalts of central Australia; the 230-Ma Wrangellia accreted oceanic plateau of western Canada; the 200-Ma Central Atlantic Magmatic Province event; the 165-Ma Rattray Formation volcanics of the North Sea Basin, Europe; the 115-Ma Kerguelen event (and its effect on northeastern India); the 65-Ma Deccan event of India; and the 60-Ma North Atlantic Magmatic Province. Şengör (2001) reviewed the uplift associated with small plumes in northern and central Africa, which are inferred to rise from mid-mantle depths. These have also been linked to the Afar plume by lateral sublithospheric channeling (Ebinger & Sleep 1998).

In some cases, magma generated above the plume center is efficiently transferred laterally away from the center of uplift via dykes or sills within or at the base of the crust (e.g., Ernst & Buchan 1997b, Wilson & Head 2002). Removal of magma from the central region has the effect of compensating for the upward movement produced by the underlying buoyancy of the plume (Campbell 2001). An example might be the 250-Ma Siberian Traps, which appear to lack associated uplift (Czamanske et al. 1998).

In reality, uplift above a plume may be more complex than the simple model described above and illustrated in Figure 1*B*. Complications include the possible presence of elongated uplift related to "hot lines" (Figure 1 in White & McKenzie 1995), the variation in topography as the plume flattens and expands beneath the lithosphere (Griffiths & Campbell 1991), the changing size of the swell depending on the depth at which the plume head stalls (shallower underneath oceanic than under continental lithosphere), and the effect of lithospheric "thin spots." The plume head may slide upward along a lithospheric root and ascend into a lithospheric thin spots (Thompson & Gibson 1991), in which case the shape of the hole will control the shape of the uplift. A study of the Iceland plume (White & Lovell 1997) suggested a correlation between pulses of clastic sedimentary input into surrounding basins and pulses of plume-generated magmatic underplating and uplift. As a further complication (W. Bleeker, personal communication, 2002) it may be difficult in poorly exposed sequences to distinguish rift flank uplift (e.g., Menzies et al. 2002b) from plume-induced domal uplift.

Rifts and Breakup Margins

The classic model of Burke & Dewey (1973) links triple junction rifting [rift stars in the terminology of Şengör (1995) and Şengör & Natal'in (2001)] to continental breakup or attempted breakup above a mantle plume. A recent review by Şengör & Natal'in (2001) identifies 567 rifts. These authors use several systems to classify the rifts. The geometric classification includes solitary rifts, rift stars, and other more complicated patterns. Kinematic classification is on the basis of plate tectonic setting and includes intraplate rifts as well as those associated with divergent, conservative, and convergent plate boundaries. Dynamical classification consists of rifts related to passive (plate tectonic) or active (plume upwelling) forces. Şengör & Natal'in (2001) consider all those rifts from an intraplate setting that exhibit uplift prior to rifting or that are linked with dynamic uplift to be of plume origin. They catalogued 181 rifts (or 32% of the total) that are plausibly plume related. In addition, we would consider any rift stars to be plume related, even if there is no prior uplift, provided they are associated with a LIP. According to Campbell (2001), plume magmatism can occur without uplift when the area covered by the magmatism is much greater than the area drained in the mantle. However, in a plume setting, any uplift must always precede volcanism. The LIP association with such rifts is important because propagating rifts (of nonplume origin) can bifurcate and the point of bifurcation can potentially be mistaken for a rift star (W. Bleeker, personal communication, 2002).

The Şengör & Natal'in (2001) catalogue does not include rifts that have been inverted or destroyed during subsequent deformation events. Therefore, their database focuses on the younger, better-preserved record. Nevertheless, applying their classification system to the older record would suggest that at least 30% of rifts are plume related. To summarize, rifts can be linked to plumes using the following criteria: an intraplate setting, an association with domal uplift, and/or a triple junction rift (rift star) geometry.

In addition, because plume-generated rifting is frequently associated with continental breakup (e.g., Hill 1991, Courtillot et al. 1999, Ernst & Buchan 2001c), it is important to investigate continental breakup margins throughout the geologic record for plume involvement. The rationale and methodology are as follows: Ninety percent of present-day passive margins around the world are associated with volcanism and can be considered volcanic rifted margins (VRMs) (Menzies et al. 2002b). In the young record, many VRMs can be linked to plume-generated LIP magmatism, although magma sources for other VRMs may reside in the shallow mantle and be associated with asthenospheric small-scale convection (e.g., Menzies et al. 2002b). Plume-associated VRMs may postdate flood volcanism (LIPs) but predate ocean opening and formation of true oceanic (MORB) crust (Menzies et al. 2002b). For example, most of the continental margins bordering the Atlantic ocean are VRMs associated with either the 200-Ma CAMP (Central Atlantic Magmatic Province), 133-Ma Paraná-Etendeka, or 62-Ma NAIP (North Atlantic Igneous Province) plume events. Examples of nonvolcanic margins include

southeast China, Iberia, the northern Red Sea, and Newfoundland Basin/Labrador Sea. VRMs can be recognized by a seaward-dipping reflector series (SDRS), and also by a significant thicknesses (up to 15 km) of juvenile high-velocity lower crust (HVLC) located seaward from the continental rifted margin (Menzies et al. 2002b).

More speculatively, an additional type of extensional structure, an "apical" graben a few hundred kilometers across (similar to a large caldera collapse structure), has been tentatively identified above the plume center region of the Mackenzie event (Figure 2*B*) (Baragar et al. 1996).

Compressional Structures

Compressional structures are important in subduction and continental collision settings but are not usually linked with plumes. An exception is Passchier's (1995) work in the Yilgarn craton, which linked contemporaneous early extension and thrusting with the plume model of Campbell & Hill (1988) for generation of the 2.7-Ga greenstone belts. One potential caveat with the Yilgarn craton example is the difficulty of generating peripheral compressional structures in a setting that was dominantly subaqueous (W. Bleeker, personal communication, 2002).

A more general analysis of compressional structures associated with plumes was recently presented by Mège & Ernst (2001) and was prompted by work on the Tharsis volcanic province of Mars (Mège 2001). The 5000-km wide Tharsis plume province is completely circumscribed by a set of wrinkle ridges (on the flanks of the uplift) and also by a set of peripheral thrust belts at the edge of the uplift. Similarly, on Venus some wrinkle ridge populations circumscribe young plume-generated uplifts (called "volcanic rises"). However, multiple origins for the wrinkle ridges appear likely, and indeed the wrinkle ridges of the volcanic plains on Venus appear to be globally synchronous. They may have a nonplume origin, and, in particular, may have originated because of density changes (expansion) of surface units as the atmosphere warmed to the current $>460^{\circ}$C surface temperatures (Solomon et al. 1999).

On Earth, wrinkle ridges have been described in association with the Columbia River and North Atlantic Igneous Province LIPs (Mège & Ernst 2001). Peripheral thrust belts have been interpreted for the Yilgarn craton greenstone belts (Passchier 1995, Mège & Ernst 2001; note caveat given above regarding this example), and have been modeled for the edge of the uplift associated with the 1270 Ma Mackenzie dyke event (Figure 2*B*) in order to accommodate the unrealistic uplifts implied by dyke intrusion density associated with a purely vertical uplift (a problem identified in Baragar et al. 1996).

DEEP CRUSTAL AND UPPER MANTLE EVIDENCE FOR PLUMES

We now turn to the evidence in the deep crust and upper mantle for the presence of ancient "fossil" plume heads.

Subcretion of Fossil Plume Heads to the Lithosphere

Plume heads that have been accreted to the lithosphere and are now traveling with their host plate will continue to influence subsequent magmatism (Condie 2001, pp. 185–86). For example, the source of basalts in the Arabian-Nubian shield for the past 900 Ma may have been a fossil plume head that was accreted to the lithosphere during the formation of the Arabian-Nubian shield (Stein & Hofmann 1992; Condie 2001, p. 186). More generally, using geochemical criteria, Condie (2001, p. 186–90) suggests that a minimum of one third of the lower crust dating from post-Archean time comprises mafic rocks from plume sources, either as accreted oceanic plateaus or as underplated mafic magmatism. Indeed, it is possible that subcretion of plume heads is a mechanism for lithospheric growth (Condie 2001). There are several emerging strategies for identifying subcreted fossil plume heads.

Lower Crustal Xenoliths

One technique is to identify lower crustal mafic xenoliths that can be linked with regional mantle plume events. For example, mafic xenoliths from young Phanerozoic kimberlites of the Lac de Gras area of the Slave Province of northern Canada contain zircon (and rutile), which yield both Archean and Proterozoic ages. The Proterozoic ages are similar to the postcratonization 1.27-Ga Mackenzie and 2.23–2.21-Ga Malley and MacKay dyke swarms, which are prominent in the same region (Davis 1997). The giant radiating Mackenzie dyke swarm is a well-characterized plume event, whereas the plume origin of the Malley and MacKay dykes is speculative (Ernst & Buchan 2001b).

Another example is from the Kirkland Lake area of the Abitibi belt of the Superior Province of Canada. A kimberlite pipe yielded xenoliths with Archean and 2.4–2.5-Ga zircon ages. The latter are similar to the regionally distributed Matachewan plume event (Moser & Heaman 1997).

These metamorphic zircon (and rutile) ages from the Slave and southern Superior Provinces of Canada are interpreted as evidence for thermal pulses due to intrusion of plume-generated magmas along the crust-mantle interface, and point to the existence of a nearby (underlying?) plume head.

Seismic Imaging of Subcratonic Mantle

Slow seismic anomalies are located in the mantle lithosphere immediately beneath the Paraná (VanDecar et al. 1995), Deccan (Kennett & Widiyantoro 1999), and Ontong Java LIPs (Richardson et al. 2000, Klosko et al. 2001). Two of these are preserved beneath continental lithosphere, whereas the third is wholly beneath oceanic lithosphere. In each case, the slow seismic anomaly extends down to great depths: 500 km (Paraná), 250 km and possibly 500 km (Deccan), and 300 km (Ontong Java). Anomaly widths are 300 km (Paraná), 800 km (Deccan), and 1200 km (Ontong Java). These seismic anomalies can be interpreted as fossil mantle-plume heads, which represent a combination of a residual thermal anomaly

and a restite root remaining after partial melt was extracted over this depth range to produce the overlying flood basalt province. Evidence suggesting that the anomaly is at least partially chemical in nature is provided by Ontong Java, where the seismically slow region is seemingly strong enough to perturb asthenospheric flow (Klosko et al. 2001). If these results can be generalized, then sublithospheric mantle can be scanned for slow seismic anomalies that might mark the presence of fossil plume heads traveling with the overlying plate. However, given that thermal anomalies will persist for only 500–1000 Ma (Griffiths & Campbell 1990, Campbell 2001), recognition of Proterozoic and Archean fossil plume-heads depends on the existence of a persistent compositional anomaly.

It is also possible that a circular distribution of lower crustal and upper mantle geophysical anomalies can point to the presence of mantle plumes. Work by Orovetskii (1999) in the Ukrainian Shield using data mainly from the 1960s and 1970s, identified "transcrustal geophysical anomalies" on a scale of a couple of hundred kilometers across and linked them to mantle plumes. The analysis is interesting but needs to be repeated using more modern datasets.

Xenoliths from the Subcratonic Lithospheric Mantle

The arrival of mantle plumes at the base of the lithosphere and associated erosion of lithosphere should leave some record that can be used in the search for ancient plumes. Indeed, subcretion of plume residue after partial melting may help form Archean continental lithospheric roots (e.g., Wyman & Kerrich 2002). The temperature, pressure, and composition of the subcontinental lithosphere mantle (SCLM) can be mapped using xenolith "probes" found in kimberlites. Geothermobarometry can be determined using Ni in garnet and Zn in chromite (Griffin et al. 1999). Furthermore, the Cr and Ca contents in the garnets can be used to infer the whole-rock mineralogy (i.e., whether the rock is lherzolite, Ca-harzburgite, low-Ca harzburgite, wehrlite, websterite, etc.). Thus, temperature, pressure, and composition can be determined as a function of depth beneath kimberlite pipes. From the regional distribution of these parameters, a three-dimensional picture of the subcontinental mantle can be determined and analyzed for anomalies that could be linked to fossil plume heads.

Although such studies are still in their infancy, exciting results have already been obtained from the Slave craton of the northern Canadian Shield. Based on analysis of >1100 garnets and >600 chromites from 21 kimberlite intrusions, Griffin et al. (1999) has shown that the mantle beneath the Lac de Gras area of the Slave craton is strongly stratified with an ultradepleted shallow layer (>100–140 km), possibly representing underplating by a subducting slab, and a less depleted deep layer (140–200 km), possibly plume derived.

Furthermore, the subsequent (postcratonization) evolution of lithospheric mantle can be monitored by PGE and Re/Os isotopic analyses of peridotite xenoliths in kimberlites (e.g., Pearson 1999). For example, case studies from northern Canada provide evidence for modification of lithospheric roots by subsequent subduction

and (of most importance for the present review) by subsequent mantle plume events (Irvine et al. 2003).

LOCATION AND SIZE OF A MANTLE PLUME

There are three geographic elements that are important for establishing the location and size of a mantle plume: the center of the plume head, the center of the plume conduit, and the trace of the plume head's outer boundary (Figure 1*B*).

Locating the Center of a Plume Head

In general, the center of the plume head will be beneath the center of the associated topographic uplift. Another possible method of determining the location of the plume-head center (Figure 1*B*) involves examining the distribution of plume-related magmatism (in a predrift configuration). A simple approach is to circumscribe the magmatism and take the center of the distribution to overlie the plume center. This is essentially the technique used by White & McKenzie (1989) for Mesozoic/Cenozoic LIPs. However, as noted earlier, magma may be transported by dykes far beyond the region of the plume center, making the method less reliable. A more definite approach for locating plume centers is to use giant radiating dyke swarms whose focal point marks the plume center (e.g., Ernst & Buchan 2001) (Figure 2*B*). Also, paleocurrent patterns and incised canyons will radiate away from the uplifted plume center (Cox 1989, Williams & Gostin 2000, Rainbird & Ernst 2001) as will triple junction rifts (rift stars) (Burke & Dewey 1973, Şengör & Natal'in 2001).

Another potential tool is the location of picrites and komatiites. They are generated within the hot central portion of the plume head and also in the plume tail (Campbell 1998), and thus might be expected to overlie the central region (Figure 1*B*) of an underlying plume. For instance, picrites of the 183-Ma Karoo-Ferrar event have been found near the Nuanetsi plume center (Eales et al. 1984). The komatiites on Gorgona Island that belong to the 90-Ma Caribbean-Colombian LIP (Kerr et al. 1997) should therefore overlie the plume center region (although this is difficult to test because of partial accretion and deformation of this LIP). Similarly, the recently discovered Song La komatiites in northwest Vietnam, which appear to be similar in age to the Emeishan LIP of China (Walker 2002), may overlie the region of the plume center. However, because basaltic liquids can move laterally in the crust via dykes, komatiite/picrite liquids could also be laterally distributed in which case they would not necessarily be localized above the plume-center region. A more systematic comparison of picrite/komatiite distributions with known plume centers needs to be carried out to better evaluate this technique.

Locating the Center of a Plume Conduit

In general, the location where the plume conduit feeds the plume head will be directly below the center of the plume, except where the plume head has slid along

a lithospheric root into a thin spot (Thompson & Gibson 1991). In this case, high-Mg magmas might be expected to be found somewhere along the track between the plume conduit and the center of the plume head.

It should also be noted that the upper end of the plume conduit, where it feeds the plume head, does not necessarily overlie the source region for the plume in the lower mantle because seismic tomography indicates that plume conduits are often inclined (e.g., Zhao 2001, Shen et al. 2002).

Locating the Edge of the Plume Head

Because of the flattening and spreading of the plume beneath the lithosphere is a dynamic process, the size of the plume head, and hence, the location of its outer edge (Figure 1*B*) will vary with time. Also, given interaction with lithospheric topography, the plume head is likely to have an irregular outline. With these caveats, we outline several strategies.

Far from the center of a giant radiating dyke swarm, the radiating pattern of dykes gives way to a subparallel pattern (Figure 2*B*). This transition is related to the increasing influence of the regional stress field compared to that of the stress field associated with domal uplift above the plume, and has been inferred to mark the edge of uplift and the approximate edge of the flattened plume head (Ernst & Buchan 1997b, 2001c). In detail, however, the thickness of the lithospheric root below which the plume is trapped may have an effect on the wavelength and magnitude of the uplift.

The pattern of interruption in sedimentation that occurs during plume arrival can be used to establish plume-head size, as first suggested by Hill (1991) (see also Rainbird & Ernst 2001). For example, the timing of sedimentation in the Newark basins of the eastern coast of North America varies with distance from the center of the 200 Ma CAMP plume. Newark basins in the south, located within 1000 km of the plume center, ceased to accumulate sediments at ca. 220 Ma. However, Newark basins from farther north along the coast, up to about 3000-km away from the plume center near Florida, do not show an interruption in sedimentation. Therefore, it can be inferred that the uplift and hence the plume head never extended beyond about a 1000-km radius. [Non-plume models for the CAMP event are discussed by Hames et al. (2003).]

Another idea worth exploring is whether carbonatites and lamprophyres are preferentially located near the cooler, more volatile-rich margins of plumes (K. Bell, written communication, 2002).

White & McKenzie (1989) looked at the main distribution of volcanics associated with the Afar, Deccan, North Altantic Igneous Province, Paraná-Etendeka, and Karoo-Ferrar LIPs and concluded that most of the magmatism in each case fits within a 1000-km radius circle, a plume size favored from theoretical considerations. This approach assumes that magma generation occurred throughout the top of the plume head. However, if magma generation was restricted to the central region of the plume head (Figure 1*B*), then the estimate of the size of plume

head based on distribution of magmatic products could be an underestimate. Alternatively, because magma can be transported laterally for long distances via dykes (e.g., Ernst & Baragar 1992, Ernst & Buchan 2001) and by sublithospheric flow (Ebinger & Sleep 1998, Wilson 1997), the areal extent of activity may overestimate the plume-head size (as mentioned above).

Finally, xenolith populations transported to the surface in kimberlites may be useful in estimating plume-head size. These can be used to map the subcrustal mantle as a function of depth (as discussed earlier), and if the kimberlites are widely distributed, their xenolith populations can potentially be used to map the extent of the underlying fossil plume head subcreted to the lithosphere.

Maximum plume head size has been estimated using the various techniques above for two of the largest continental LIPs, the 1270 Ma Mackenzie and 200 Ma Central Atlantic Magmatic Province events, as well as two of the largest oceanic LIPs, Ontong Java and Manihiki (Ernst & Buchan 2002). Each is consistent with an underlying flattened plume-head radius of about 1000 km, a value considered normal for a plume rising from the deep mantle (Campbell 2001). It is signficant that even the largest LIP, Ontong Java, which is part of a "superplume" event (see later discussion), can be generated from a flattened plume head of normal (1000-km radius) size.

ASSESSMENT OF OTHER PROPOSED INDICATORS OF MANTLE PLUMES

A number of additional criteria have been proposed for the recognition of mantle plumes. These include environmental consequences, such as changes in the isotopic composition of seawater, anoxia events, and eustatic sea level changes. It has also been proposed that major events, such as supercontinent breakup, bursts of juvenile crust production, magnetic superchrons, global extinction, and meteorite impact events, are linked to particularly significant plume events. We provide a review of each and consider the links with the plume record as recorded by LIPs.

The Problem of Different Timescales

Before attempting to compare the timing of LIP events with other possible indicators of plumes (Figure 5), we must emphasize the large uncertainties in comparing the timescales that are used in calibrating different datasets. Nearly all the LIP (plume head) events are dated isotopically, frequently to a resolution of a few million years or less, mainly using the U-Pb system. However, the seawater isotope data, as well as the sea level, impact, and extinction data for the Phanerozoic, are generally dated biostratigraphically. Therefore, the biostratigraphic data must be converted to a timescale suitable for comparison with the isotopically dated LIP record. Unfortunately, as demonstrated in Table 2, there are distinct differences between the ages assigned to stage boundaries according to the classic Harland et al. (1990) timescale and more recent revisions by Gradstein & Ogg (1996) and Okulitch (2002). Given differences of up to 10 Ma between even the more recent

timescales, the comparison between the different datasets in Figure 5 must be viewed as preliminary.

Environmental Effects: Seawater Composition (Sr, C, and O isotopes), Anoxia, and Sea-Level Rise

THEORETICAL LINKS The isotopic composition of seawater is sensitive to the changes in global magmatic/tectonic activity and can be monitored through the isotopic fluctuations in the marine carbonate record (e.g., Veizer et al. 1999). For example, oceanic plateaus release Sr into the ocean through hydrothermal brine exchange between seafloor basalts and the ocean, and continental LIPs release Sr into the ocean through weathering and transport by rivers. A LIP event, whether oceanic or continental, should shift the $^{87}Sr/^{86}Sr$ ratio to lower, more mantle-like values, i.e., produce a negative Sr isotopic excursion.

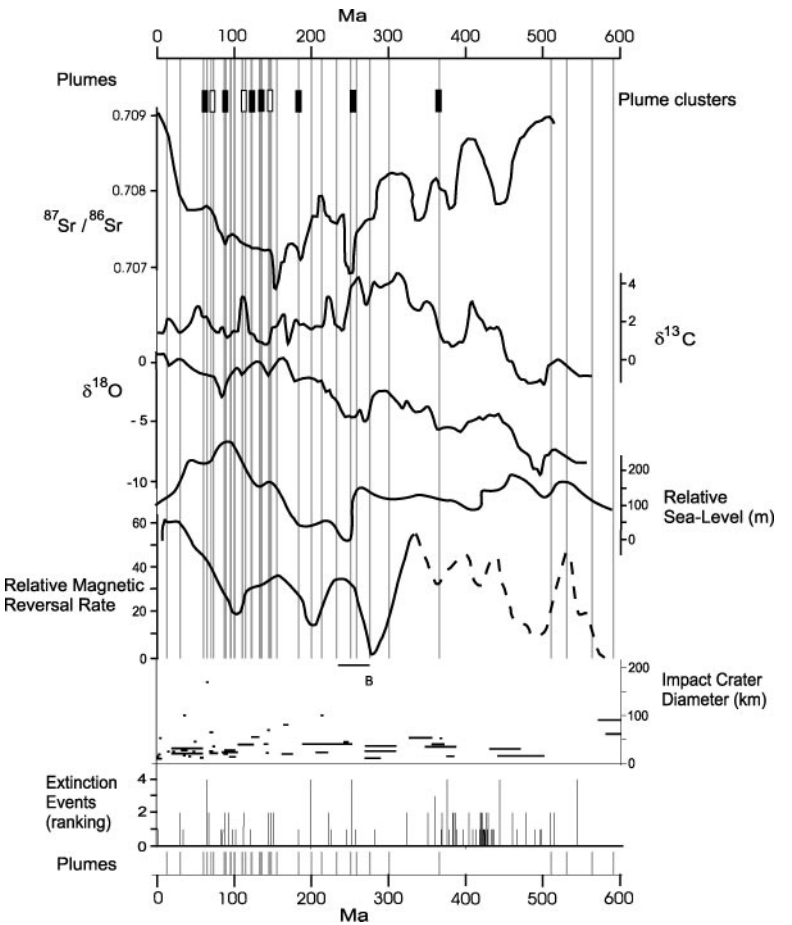

Global warming due to CO_2 is transient. Weathering and erosion of the LIP causes a net reduction in CO_2 and increased organic productivity, and burial rates cause large-scale deposition of black shales and, hence, a ^{13}C-enriched ocean (Kerr 1998, Condie et al. 2001). This also leads to global cooling (a mini–ice age) a few million years after initiation of the LIP event (Wignall 2001, Chumakov 2001). Also, SO_2 release from the LIP will produce a transient cooling (Wignall 2001).

The oxygen isotope record ($^{18}O/^{16}O$) is primarily a measure of paleotemperature and will respond to a LIP event with increased sea-surface temperatures (lower $\delta^{18}O$) owing to CO_2 release and global warming. For example, the eruption of Deccan Traps may have produced a greenhouse effect of 2°C (Caldeira & Rampino 1990), whereas the Mid-Cretaceous superplume event could have raised temperatures by 8°C (Barron et al. 1995, Caldeira & Rampino 1991) as summarized by Condie (2001, p. 251). However, the magnitude of the thermal excursion will generally be small unless the modest temperature increase (and uplift) due to the plume also destabilizes methane hydrate (clathrate) mega-reservoirs causing massive release of the greenhouse gas, methane (e.g., Wignall 2001, Jahren 2002).

In addition, the improving Os isotopic record of marine sediments has the potential to provide an additional monitor for the contribution from mantle sources (Peucker-Ehrenbrink & Ravizza 2000).

←

Figure 5 Comparison of the mantle plume record from LIPs for the Phanerozoic with other potential indicators of plume activity. The LIP record of mantle plumes (Figure 3) (Ernst & Buchan 2001b) is given by grey vertical lines (labeled plumes). Events occuring on more than one continental block that may represent plume clusters ("superplume" events) are indicated with boxes. Solid boxes are well dated; unfilled boxes have 2σ age uncertainties of >10 Ma. Seawater isotopic composition (Sr, O, and C) curves are after Veizer et al. (1999). Specifically, the minimum Sr-isotope values at each age were chosen, whereas for O and C isotopes, the mean values at each age were used. The sea-level curve is from Figure 9.2 in Condie (2001), whereas the relative magnetic reversal rate is modified from Johnson et al. (1995). All these datasets were plotted according to the Harland et al. (1990) timescale because that was how they were presented in the original papers (see Table 2). The extinction events are ranked by their significance according to the four-part classification of Barnes et al. (1996), their ages assigned according to the Okulitch (2002) timescale. The most recently published meteorite impact database is from Grieve & Shoemaker (1994). However, the impact database is rapidly changing and the data in Figure 5 was extracted in June 2002 from the website maintained by the University of New Brunswick (Earth Impact Database 2002). To this database has been added the Bedout (B) and Alamo impacts. Uncertainties were generally at the one sigma level. Uncertainties for the Azuaga (∼40 Ma), Bedout (∼255 Ma), Alamo (367 Ma), Slate Islands (∼450 Ma), Acraman (∼590 Ma), and Beaverhead (600 Ma) impacts were not available on the website, and for these, an uncertainly of +/−20 Ma was arbitrarily assigned. Toms Canyon was assigned an age of 35 Ma (based on Poag 1997).

TABLE 2 Timescale comparison

	H[a]	Difference between H and G	G[b]	Difference between G and O	O[c]	Difference between H and O
Neogene	23.3	0.5	23.8	0.9	22.9	0.4
Paleogene	65.0	0.0	65.0	0.0	65.0	0.0
Cretaceous	145.6	3.6	142.0	2.8	144.8	0.8
Jurassic	208.0	2.3	205.7	5.7	200	8.0
Triassic	245.0	3.2	248.2	4.8	253	8.0
Permian	290.0	0.0	290.0	10.0	300	10.0
Carboniferous	362.5	8.5	354.0	6.0	360	2.5
Devonian	408.5	8.5	417.0	1.0	418	9.5
Silurian	439.0	4.0	443.0	0.0	443	4.0
Ordovician	510.0	15.0	495.0	6.0	489	21.0
Cambrian	570	25	545.0	1.0	544	26

[a]Harland et al. 1990.

[b]Gradstein & Ogg 1996.

[c]Okulitch 2002.

Arrival of a mantle plume beneath oceanic lithosphere should result in a rise in eustatic sea level (e.g., Kerr 1998, Condie et al. 2001). Sea level rises because of isostatic uplift and thermal erosion of the oceanic lithosphere above plume heads (Kerr 1998, Lithgow-Bertelloni & Silver 1998) and displacement of water by the oceanic LIP itself. For example, emplacement of the Ontong Java LIP would cause an estimated sea-level rise of at least 10 m (Coffin & Eldholm 1994), although there remain considerable uncertainties in the uplift history of this LIP (Neal et al. 1997).

One potential method of distinguishing which eustatic sea-level rises are linked to mantle plumes may be provided by the iron formation record. Isley & Abbott (1999) and Abbott & Isley (2001) have suggested that iron formations can be linked to the presence of oceanic plateaus (as the source of iron) and sea-level rise (increasing the extent of shallow marine shelves available for deposition of iron). However, large dating uncertainties for iron formations currently limit the use of the iron formation record for recognizing plume events.

Locally, the arrival of a plume beneath continental lithosphere will contribute to sea-level fall owing to domal uplift above the plume. However, on a global scale, continental plumes will contribute to sea-level rise providing the plume can be linked with continental breakup and the formation of extensive new buoyant

oceanic crust and lithosphere causing widespread transient flooding of shallow platform environments and sedimentary transgression onto the continents.

COMPARISON WITH THE LIP RECORD The recently available "Bochum/Ottawa Isotope Dataset" of Phanerozoic seawater curves for $^{87}Sr/^{86}Sr$, $\delta^{18}O$, and $\delta^{13}C$ (Veizer et al. 1999, Prokoph & Veizer 1999) are compared with our LIP record in Figure 5. In general, the first-order decreases in Sr (reflecting increased mantle contribution), increases in $\delta^{13}C$ (reflecting fixing of atmospheric CO_2), and decreases in $\delta^{18}O$ (reflecting temperature increase) do not strongly correlate with the LIP pattern, which suggests that plume-related effects can be masked by broader controls related to continental breakup and assembly and to climatic effects. In the more detailed discussion below, it is necessary to remember the problems associated with mixing isotopic and bistratigraphic timescales that were described above.

Major troughs in the $^{87}Sr/^{86}Sr$ isotopic curves at 160, 190, and 260 Ma are matched by LIP events, but the troughs at 330, 380, and 450 Ma do not correspond with known LIPs. Furthermore, many known LIPs do not correspond with troughs, although the 280- and 200-Ma LIPs may correspond with inflections in the data. In any case, additional controls, such as the variation in sea-floor spreading rate, may exert a more significant control.

Times of increased burial of carbon (marked by positive excursions of $\delta^{13}C$, i.e., increases in the $^{13}C/^{12}C$ isotopic ratio) are observed at numerous times in Figure 5. However, only the increases at about 17 and 110 Ma and inflections in the curves at 145 and 250 Ma correspond to LIP events.

Temperature increases (depleted values of $\delta^{18}O$, i.e., decreases in the $^{18}O/^{16}O$ isotopic ratio) match only a few LIPs, at 110 and 140 Ma, and perhaps at 90 Ma and 250 Ma. Clearly, other controls related to climate are more significant in controlling the $\delta^{18}O$ fluctuations.

The eustatic sea-level curve shows a broad 400-Ma cyclicity (Worsley et al. 1986) with second-order peaks at 530, 480, 270, 220, 160, and 100 Ma, and minor peaks at 420 and 60 Ma. These only broadly correlate with timing of LIPs. The additional complexities reflect other factors, in addition to mantle plume arrival, that contribute to sea-level uplift. There is potential that these factors may be distinguished on the basis of duration. For example, glacial events operate on timescales of ten thousand to a million years, whereas continent breakup and collisional events operate on a timescale of 1 to 100 Ma.

Global Extinction Events and Meteorite Impacts: Comparison with the LIP Record

A heated debate has raged for more than two decades over whether global extinctions are caused by meteorite impacts or LIP events. Those supporting the impact connection cite the close correspondence in age between the large Chicxulub impact, associated large iridium anomaly, and the K-T extinction event that marked the end of the age of dinosaurs (e.g., Alvarez et al. 1980, Hildebrand et al. 1991). Other correlations between large impacts and extinctions are less clear because of

the uncertainty in the ages of most large impacts, or in some cases, because of uncertainty in the age of the extinction events (see Figure 5). In some cases, it has been proposed that multiple impacts are required for an observable effect, and that the extinction event itself lags the impacts by several million years (e.g., McGhee 2001).

On the other hand, supporters of a LIP-extinction connection propose that several of the LIPs in the past 250 Ma are similar in age to important extinction events (e.g., Courtillot 1996, Wignall 2001). They also argue that many extinction events do not begin as suddenly as expected under the impact hypothesis. They conclude that LIP events and their climatic affects are the most likely cause of global extinctions.

The LIP database of Ernst & Buchan (2001b), coupled with the most recent version of the Earth Impact Database (2002) allows a more robust age comparison between LIPs, extinctions, and impacts than previously available, especially for the 600–250 Ma period (Figure 5). However, once again, the difficulties associated with the timescales that are based on a mix of isotopic and biostratigraphic ages must be kept in mind.

Some LIPs are readily correlated within several million years or less with global extinctions (Figure 5) (Courtillot 1996, Wignall 2001). For example, the Deccan Traps, CAMP event, and Siberian Traps are similar in age to the Cretaceous-Tertiary, Triassic-Jurassic, and Permian-Triassic boundary extinctions, respectively. Other LIP events, however, are not correlated with major extinctions. For example, there is no Early Cretaceous (Aptian) global extinction to match the huge Ontong Java oceanic plateau, and no 300 Ma extinction corresponding to the Jutland LIP event. On the other hand, some large Paleozoic extinctions, including the Ordovician-Silurian boundary extinction, have yet to be correlated with LIPs. In addition, where a LIP-extinction correlation does exist, the eruption volume of the LIP appears unrelated to the intensity of the extinction event (Wignall 2001).

A resolution of the controversy as to whether LIPs or impacts are responsible for extinction events has been proposed in which impacts are responsible for triggering LIP events (Rampino & Stothers 1988, Isley & Abbott 2002, Jones et al. 2002). However, the ability of an impact to cause flood basalt magmatism has been questioned by the analyses of Loper & McCartney (1990) and Melosh (2001).

Much more information is required before a clear picture of the correlation between meteorite impacts, LIPs, and global extinctions over the past 600 Ma emerges. Perhaps more attention needs to be directed toward the possibility that global extinctions may be caused by more than one mechanism, and that even individual extinction events may have multiple causes.

RECOGNITION OF "SUPERPLUME EVENTS"

Present-day Pacific and African deep-mantle upwellings have been linked with clusters of LIPs spanning tens of millions of years and have been interpreted to represent "superplumes" (Maruyama 1994, Fukao et al. 1994), "superplume

events" (Condie 2001), "megaplumes" (Storey & Kyle 1997, Forte & Mitrovica 2001), or "superswells" (McNutt 1998, Davies 1999). The Pacific and African superplume events are also linked with broad geoid highs (Crough & Jurdy 1980), and may be long-lived features, having originated during prior breakup of the supercontinents, Rodinia (at about 700 Ma) and Gondwanaland (200 Ma), respectively (Pavoni 1997). The Pacific superplume event produced the mid-Cretaceous cluster of oceanic plateaus (Larson 1991a,b), which includes the largest known LIP, the 40×10^6 km^3 Ontong Java oceanic plateau (Coffin & Eldholm 1994).

The nature of such superplume events is becoming clearer with a recent seismic study of the mantle transition-zone thickness across the South Pacific superswell that searched for thinned regions marking the passage of hot plumes (Niu et al. 2002). Niu et al. (2002) concluded that widespread volcanism across the South Pacific Superswell is primarily an upper-mantle phenomenon and probably reflects somewhat higher temperatures and melt generation rates than normal, except for the presence of at least one narrow plume originating from the lower mantle. This is consistent with the model for a superplume event as a broad upwelling in the mantle ("superswell"), through which individual normal-sized deep-mantle plumes rise (e.g., Davies 1999). The upwelling may develop as a counter flow to flanking subduction zones.

How can superplume events be recognized in the older record, and are they linked to past episodes of supercontinent breakup (Li et al. 2003), bursts of juvenile crust production associated with supercontinent formation events (e.g., Condie 2001), and times of magnetic superchrons? We consider each of these in turn, and first begin with the LIP record as a guide to the recognition of larger-than-normal events, i.e., "superplume events." In particular, we focus on the idea of plume clusters.

Recognizing "Superplume Events" (i.e., Plume Clusters) in the Older Record

Superplume events can be recognized as clusters of plumes in the geologic record (Ernst & Buchan 2001b, 2002; Condie 2001). Plume clusters are most easily recognized in the Mesozoic/Cenozoic record. However, more ancient plume clusters are difficult to recognize because of our poor understanding of Precambrian and Paleozoic paleocontinental reconstructions (Ernst & Buchan 2002).

At several times since 600 Ma, multiple LIPs whose ages span 10 Ma or less can be linked to more than one plume center (Figure 3) (Ernst & Buchan 2002). In some cases (e.g., the 183-Ma Karoo-Ferrar event), the different plumes are sufficiently close to one another to be plausibly derived from a common deep-mantle upwelling. However, other coeval plumes (e.g., marked by the 65-Ma Deccan flood basalts of India and the 62-Ma North Atlantic Igneous Province of the United Kingdom and Greenland) are more than 10,000 km apart at the time of their nearly simultaneous emplacement and likely represent independent deep-mantle events. At about 45 times since 3.0 Ga, LIPs are found on more than one continental block

(Figure 3) and may represent plume clusters (or superplume events). However, better-constrained continental reconstructions are required in order to determine which of these are due to tectonically fragmented single plumes and which require multiple plumes. Therefore, the use of plume cluster criteria to recognize superplume events must await integrated paleomagnetic and geochronologic studies to define the past reconstructions of continents.

Links with Environmental Effects?

It is probable that the occurrence of plume clusters will have a greater effect on seawater composition, sea level, and other aspects of the marine sedimentary record than that of a single plume. The timing of potential plume clusters (Figure 3*C*) are compared with these other data types in Figure 5. There is no obvious correlation between the timing of potential plume clusters and the Sr, O, and C isotopic curves, suggesting that other controls on isotopic composition, such as supercontinent breakup, production of new buoyant crust, accretion of blocks into continents, and glacial events (e.g., "Snowball Earth"), complicate the recognition of the plume-cluster effect.

Links with Supercontinent Breakup?

It has been widely inferred that the breakup of supercontinents is associated with clusters of plumes. Specifically, the breakup of Gondwanaland between 180–65 Ma has been linked to plume-head events at 183, 145, 135, 90, and 65 Ma (Storey 1995), and the breakup of Rodinia in stages by plumes at 825, 780, and 755 Ma (Li et al. 2003). The formation of the Iapetus Ocean is marked by magmatic events from 615 to 550 Ma, which may represent three plumes (events 52–54 in Table 1 of Ernst & Buchan 2001b). However, during, and between each of these plume-cluster intervals, there were other important plumes that rose beneath continental lithosphere but were apparently not linked to breakup. For example, the Siberian Traps (250 Ma) and the Antrim basalts (510 Ma) of Australia (Figure 2*A*) represent major LIP events not linked to breakup. So it is not clear whether supercontinent breakup represents a time of enhanced plume activity or whether it simply represents a plate-stress configuration that is favorable for plume-assisted breakup. These periods of more widespread extensional environments might favor more extensive partial melting of plumes that produce larger and therefore better-preserved LIPs.

Links with Subducted Slabs?

Plumes can be linked with the distribution of pre-existing subduction zones. For example, geochemical evidence (discussed earlier) indicates that plume source regions contain a significant subducted component (as the source for OIB components: EM1, EM2, and HIMU) (e.g., van Keken et al. 2002). Plume clusters (superplume events) may, therefore, be linked with large-scale patterns of subducted

slabs. For example, a concentration of subducted slabs (a slab "graveyard") beneath an amalgamating supercontinent may represent a source of eclogite and, more controversially, subducted water that would contribute to the ascent of plumes in these regions a few hundred million years later (Maruyama 1994, Fukao et al. 1994, Windley & Maruyama 2002).

Another type of link between subducted slabs and plume clusters is the following. Consider a large tectonic plate, either a supercontinent, such as Gondwanaland, or a large oceanic plate, such as the present-day Pacific plate. Subduction around the periphery of a large plate will result in cooling around its edges, but the central region under the plate will remain warmer. This may result in an upwelling in the intervening central region, which produces a geoid high (Lowman & Gable 1999). The formation of such broad mantle upwellings can cause thickening of the D″ layer, and the ascent of multiple plumes (Davies 1999). A similar model was obtained in the numerical modeling of Tan et al. (2002) who conclude that plumes are preferentially generated on the edge of deeply subducted slabs. In addition, beneath slabs, a substantial amount of hot mantle can be trapped over long periods of time, leading to "mega-plume" formation. According to these models, the distribution of fossil subduction zones can potentially be a guide to the location, timing, and scale of subsequent plumes.

Links with Formation of Juvenile Crust?

Condie (2001 and references therein) has proposed that peaks in the production of new juvenile crust represent superplume events. The formation of juvenile crust has been strongly episodic through time, with major peaks in production at 2.7–2.6 and 1.9–1.8 Ga and minor peaks at 2.9–2.8, 0.6–0.5, 0.4–0.3, and 0.2–0.1 Ga (Figure 8.8 in Condie 2001). Condie (2001) proposed that the increased rate of subduction is linked to a superplume event via a mantle avalanche event wherein subducted slabs that have temporarily stalled at the 660-km boundary, suddenly breach the transition zone and descend to the base of the mantle. This in turn initiates an upward counterflow of mantle and the rise of numerous plumes.

The oceanic record is key to testing the proposed link between superplume events and peaks (mainly at 2.7 and 1.9 Ga) in the production of juvenile crust. Specifically, oceanic plateaus and mafic underplating (both produced by plumes) can potentially contribute to the formation of new crust during collisional events. In a plume context, the bursts in juvenile crust formation either represent higher than normal rates of oceanic plateau production or increased rates of plate convergence, which results in more efficient obduction/underplating of oceanic plateaus during continental accretion. However, the recognition of accreted oceanic plateaus in 2.7-Ga juvenile crust has become more uncertain as discussed earlier, because a (para)authochthonous setting for greenstone belts seems to be common (Bleeker 2002). Furthermore, a recent review by Condie (2002) of the character of 1.9-Ga

juvenile crust indicates little presence of oceanic plateaus, and hence, no apparent plume (or superplume) role.

Links with Fluid Dynamics of the Core?

It has been proposed that the changes in the circulation pattern in the core can be linked with superplume events. One possible way of making this link is by comparing the ages of plume-derived LIPs with the ages of magnetic superchrons (e.g., Condie 2001).

Larson & Olson (1991) pointed out that the 120–80-Ma Pacific superplume event correlates with the Cretaceous normal magnetic polarity superchron. They proposed that plumes leaving from the base of the mantle cool the adjacent outer core and thus increase core circulation. This in turn stabilizes the circulation against instabilities that cause reversals of the magnetic field. Although several important Phanerozoic LIP events (the 122-Ma Ontong Java, 200-Ma Central Atlantic Magmatic Province, 280-Ma Tarim Block, 360-Ma East European craton, 360-Ma Yakutsk, and 510-Ma Antrim) (Ernst & Buchan 2001b) broadly correspond to lows in the record of reversal frequencey in Figure 5, most LIP events are not correlated with reversal rate lows. Therefore, no clear link between LIPs and magnetic reversal rate (or circulation in the core) emerges from the existing Phanerozoic data.

The Precambrian paleomagnetic record remains too discontinuous (e.g., Buchan et al. 2001) to identify earlier superchrons. However, there may be periodic fluid dynamic events in the core that cause the termination of superchrons and resumption of reversal patterns (Greff-Lefftz & Legros 1999). The interaction of core rotation and solar-lunar tidal waves predicts periodic resonances. These cause a temperature pulse that can destabilize the "D" layer and arguably spawn major plume events (Williams 1994, Greff-Lefftz & Legros 1999). Numerical modeling predicts resonances lasting 200–300 Ma at about 3.8, 3.0, 1.9, and 0.5–0.3 Ga. The 3 Ga and 1.9 Ga resonances have been linked with bursts of juvenile crust production at 2.7 and 1.9 Ga, and the Paleozoic resonance has been variably linked with the 250 Ma Siberia trap event (Greff-Lefftz & Legros 1999), major 380–360 Ma plume magmatism (Isley & Abbott 2002), or ~500-Ma Iapetus rifting (Williams 1994). Although the theoretical links between fluid dynamics in the core and superplume events seem significant, the comparison of resonance events with the plume record of Figure 3 indicates that many plume clusters (superplume events) also occur outside resonance times.

CONCLUSIONS

Mantle plumes are currently a major research focus, and recent literature links them to a wide range of global phenomena. However, most of the current work is concentrated in the late Phanerozoic and late Archean. To properly assess the role of mantle plumes in Earth history, it is essential to expand our understanding of plume events. Our goal in this review has been to consider the repertoire of techniques

available to identify plumes in order to support their expanded recognition and characterization.

The arrival of mantle plumes from the deep mantle can be convincingly recognized through large volume–short duration (<10 Ma) magmatic events, so-called LIPs. In the older record, where the flood basalt signature is lost, the identification of giant dyke swarms and the presence of high-Mg rocks (picrites and komatiites) is key. Furthermore, small volume melts, carbonatites, and kimberlites may, in some cases, be indicative of plumes. Although complicated, the application of geochemical criteria, particularly involving incompatible elements (such as the REE, and Nb-Ta) and isotopes (notably of He and Os), can help distinguish plume-related magmatism, identify the component mantle sources and track evolution of the mantle through time. Dynamic domal uplift above the plume and associated rifting and peripheral compressional structures can also be diagnostic. Fossil plume heads that are subcreted to the base of the lithosphere may be recognized through seismic and geochemical studies of xenolith populations in kimberlites.

Mantle plumes should have an indirect influence on the global environment. They have been linked with changes in sea water composition and eustatic sea level, deposition of iron formations, anoxia events, and global extinction events. There also are broad correlations with supercontinent breakup, bursts of juvenile crust production, and core circulation changes causing magnetic superchron events. However, our assessment of these datasets indicates that unique links between specific phenomenon, and LIP events remain generally speculative.

Further progress in the recognition of the ancient plumes requires expanded high-precision dating programs of large volume basaltic units and their associated plumbing systems. Rapidly evolving seismic tomography will eventually answer the fundamental questions of the structure of plumes and their depth of origin. Comparative study of plumes on Venus and Mars, which lack plate tectonics, should help clarify the influence of plate tectonics on plumes. Quantification of the complex environmental consequences of plumes will contribute to resolution of the relationship between extinction events, LIPs, and meteorite impacts.

ACKNOWLEDGMENTS

The ideas in this review developed mainly from working with authors of chapters in *Mantle Plumes: Their Identification Through Time* (Ernst & Buchan 2001a), and from participation in S. Maruyama's conference, "Superplume: International Workshop," held in January 2002 in Tokyo, Japan. We have benefited from extensive discussions with our colleague Wouter Bleeker regarding plumes. Useful comments on the paper by Nick Arndt, Keith Bell, Wouter Bleeker, Tim Bond, and Ian Campbell, are greatly appreciated. John Morgan is acknowledged for assistance in drafting the figures. We also thank the following, who provided digital versions of figures that we used with modification: George Williams (Figure 2*A*), Robert Rainbird (Figure 2*C*), Larry Heaman and Bruce Kjarsgaard (Figure 2*E*), and Kirsty Tomlinson and Kent Condie (Figure 4*B*,*C*). This is Geological Survey of Canada publication number 2002222.

APPENDIX 1

Evaluation of proposed methods for identifying plume heads and tails. A = highly indicative, B = probably indicative, C = of uncertain value, D = not (or probably not) indicative. More details and further referencing in text.

Method	Rating of plume link	Key references
LARGE IGNEOUS PROVINCE (LIPs) (PLUME HEAD)		
>100,000 km^2 mafic magmatism emplaced in <10 Ma	A	Ernst & Buchan 2001b, Coffin & Eldholm 1994, 2001
In the Phanerozoic: mainly oceanic and continental flood basalts		
In the Proterozoic: mainly recognized by plumbing systems of dykes, sills and layered intrusion along with erosional remnants of flood basalts		
Pyroclastics rare		
Distinct from island arc basalts (IAB), which are mainly pyroclastic rocks	B	Campbell 2001
The Siberian Traps are a rare LIP having extensive pyroclastics		
Bimodal volcanism (mafic + felsic)		
Distinct from IAB where there is no compositional gap (see felsic magmatism below)	C	Menzies et al. 2002b; Goodwin 1991
Giant dyke swarms		
Giant radiating dyke swarm	A	Ernst & Buchan 2001c
Giant linear dyke swarm (may be part of radiating swarm or may have rift or back-arc extension association)	B	Ernst & Buchan 2001c
Link with present day hot spots (via hot spot track)	A	Ernst & Buchan 2001b
High-Mg melts (picrites & komatiites)	B	Campbell & Griffiths 1992; Gibson 2002; Herzberg & O'Hara 1998, Campbell 2001
In Phanerozoic, Proterozic and most importantly in the Archean (see below)		
Plume picrites can be distinguished from arc picrites using geochemistry		
Volcanic rifted margins (see also bimodal volcanic rocks below)	C	Menzies et al. 2002b
Magmatic underplating	C	Cox 1993, Maclennan & Lovell 2002
SMALLER VOLUME MAFIC MAGMATIC EVENTS		
Mini-plume magmatism	A	Wilson & Patterson 2001, Burke 1996, Sengor 2001
e.g., Africa, Europe and eastern Australia		
Direct origin in upper mantle although ultimately may be derived from lower mantle		
Magmatism with age progression (plume tail)		
Seamount chain (in oceans)	A	Wilson 1963
Age progression on continents (e.g., Yellowstone or Anahim volcanics)	A	Parsons et al. 1998; Ernst & Buchan 2001c, Figure 17
ARCHEAN GREENSTONE BELTS OF PLUME ORIGIN		
Settings	B	Thurston & Chivers 1990, Condie 2001
Mafic plain association often with komatiites (has been interpreted as accreted oceanic plateaus; although Bleeker (2002) urges caution in identification of Archean oceanic plateaus)		
Platform association often with komatiites (interpreted as plume-generated magmas erupted through rifted continental crust)		

(*Continued*)

APPENDIX 1 (*Continued*)

Method	Rating of plume link	Key references
Distinguish marjorite garnet fractionation, Mg-silicate perovskite addition, and crustal contamination using (La/Yb)n, Nb/Nb*, Zr/Zr*, Hf/Hf*	B	Xie et al. 1993, Xie & Kerrich 1994, Fan & Kerrich 1997, Condie 2001, pp. 203–6, Sproule et al. 2002
Majorite garnet in source = high rare earth slope and negative Zr and Hf anomalies, but no effect on Nb (and Ta)		
Melting of source enriched in Mg-silicate perovskite = positive Nb, Ta, Zr, and Hf anomalies		
Crustal contamination = negative Nb and Ta anomalies		
LINK WITH ISOTOPIC RESERVOIRS (defined by Sr, Nd, Pb, Hf, He, Os isotopic ratios)		Hofmann 1997; Campbell 1998; Condie 2001; Kempton et al. 2000
Common OIB component (FOZO)	A	Hart et al. 1992, Hanan & Graham 1996, Hofmann 1997, Hilton et al. 1999, van Keken et al. 2002
Additional OIB components: EM1, EM2, HIMU	B	e.g., van Keken et al. 2002
DMM (depleted MORB mantle)	D	e.g., Hofmann 1997
Not source of plumes, but similar to FOZO		
Leakage from core (suprachondritic $^{186}Os/^{188}Os$)	B	Brandon et al. 1999
GEOCHEMICAL DIAGRAMS USEFUL FOR IDENTIFYING PLUME INVOLVEMENT		
Spider (multi-element) diagrams	B	Thompson et al. 1983, Campbell 2001, Condie 2001
OIB = enriched in LREE and other highly incompatible elements but not depleted in Nb, Ta, and Ti. However, deviations can occur due to crustal or lithospheric contributions (distinct from MORB and IAB) patterns		
Oceanic plateaus = flat REE, but link with FOZO (not DM)		
Continental flood basalts = can be similar to OIB pattern or contaminated pattern		
Ternary and X-Y diagrams		e.g., Pearce & Cann 1973, Winchester & Floyd 1997, Shervais 1982, Meschede 1986, Kerrich & Wyman 1997
To distinguish intraplate magmatism from arc basalt and to monitor effects of alteration and crustal contamination		
Some key incompatible element ratios	B	Hofmann 1997, Campbell 2002
Nb/U ~47, Ta/U ~2.7, Ce/Pb ~25, values in OIB and MORB, but values in arc setting are less		
Near chondritic Nb/La and Ce/Pb (versus low Nb/La and low Ce/Pb in IAB)		Campbell 2001
Th/Ta (e.g., in Condie diagram, Th/Ta versus La/Yb)		Condie 1997, 2001
Some key compatible trace elements	B	
High Ni at given MgO (distinguishes from MORB, which has lower Ni at same MgO)		Campbell 2001
Cr in olivine (can be >800 ppm in contrast to <800 ppm in island arc basalts)		Campbell 2001
Diagrams to illustrate depth of melting (effect of lithospheric "lid") versus degree of melting	B	Condie 2001, Lassiter & DePaolo 1997, Saunders et al. 1997
e.g., $[CaO/Al2O3]_{\text{for Mg = 8}}$ versus $[FeO]_{\text{for Mg = 8}}$		

(*Continued*)

APPENDIX 1 (*Continued*)

Method	Rating of plume link	Key references
ADDITIONAL "SETTINGS" THAT MAY BE RELATED TO PLUMES		
Ophiolites (some types)	C	Coffin & Eldholm 2001, Moores 2002
Felsic magmatism	C	Bryan et al. 2002
Rifts (with bimodal volcanism)	C	e.g., Menzies et al. 2002b, Goodwin 1991
Anorogenic chemistry	B	Föster et al. 1997
Caldera chain showing age progression (e.g., associated with Yellowstone and Afar plumes)	C	Bryan et al. 2002, this review
Carbonatites	B	Bell 2001, Bell & Tilton 2001, 2002
Some correlated with plume head events, and having OIB isotopic signature		
Kimberlites	C (B?)	Haggerty 1999
Some correlated with plume head event		
Age progression showing link with plume tail track	B	Heaman & Kjarsgaard 2000
Ore deposits		
Magmatic sulphides: PGEs and Ni-Cu	B	Pirajno 2000, Schissel & Smail 2001
Diamonds: see kimberlites above	B	
Giant hydrothermal ore deposits	C	Pirajno 2000
Anorthosites (plume models have been applied with difficulty)	C	Ashwal 1993
DYNAMIC FEATURES RELATED TO PLUMES		
Domal uplift of 1- to 2-km over an area of >500-km to 2500-km diameter	A	Sengor 2001, Campbell 2001
Radiating river patterns (in older rocks: radiating paleocurrent patterns, radiating incised canyons)	A	Cox 1989, Williams & Gostin 2000, Rainbird & Ernst 2001
Shoaling of sedimentary strata in center of uplift	A	Rainbird & Ernst 2001
Plumes arriving beneath subduction zone causing shallowing of the slab and resulting in crustal uplift	C	Murphy et al. 1998
Intracratonic sedimentary basins	B	e.g., Klein 1995, Kaminski & Jaupart 2000, Campbell 2001
Due to conductive cooling of the plume head over hundreds of millions of years		
Rifts and breakup margins		
Rift stars (triple junction rifts)—but must distinguish from bifurcating propogating rifts	A	Burke & Dewey 1973, Şengör 1995, Şengör & Natal'in 2001
Rifts associated with breakup margins	C	Menzies et al. 2002b
Aulacogens	B	Şengör 1995, Şengör & Natal'in 2001
Apical grabens (marking centre of uplift)	B	Barager et al. 1996
Compressional features		Mège & Ernst 2001
Circumferential wrinkle ridges	B	Mège & Ernst 2001
Circumferential thrust faults	C	Mège & Ernst 2001
DEEP CRUSTAL AND UPPER MANTLE EVIDENCE FOR PLUMES		
Seismic evidence for "fossil" plume head	A	vanDecar et al. 1995, Kennett & Widiyantoro 1999, Richardson et al. 2000, Klosko et al. 2001
Slow seismic signature in subcontinental lithosphere (e.g., beneath Deccan, Paraná, and Ontong Java LIPs)		

(*Continued*)

APPENDIX 1 (*Continued*)

Method	Rating of plume link	Key references
Identification of subcreted plumes Geochemical analysis of lithospheric xenoliths in kimberlites (e.g., analysis of Cr and Ca in garnet and Zn in chromite). Os isotopes are also useful.	B	Griffin et al. 1999
Magmatism in lower crust Identified by dating of lower crustal xenoliths in kimberlites	B	Davis 1997, Moser & Heaman 1997
LOCATION AND SIZE OF A MANTLE PLUME		
Locating the Plume Center Region		Ernst & Buchan 2002
Focus of giant radiating dyke swarm	A	Ernst & Buchan 2001c
Distribution of picrites and komatiites	B	Campbell 1998
Center of uplift identified by sedimentary unconformity patterns and paleocurrents	B	Rainbird & Ernst 2001
Circumferential dyke swarms	B	Ernst & Buchan 2001c
Arcuate wrinkle ridges	B	Mège & Ernst 2001
Locating the Edge of Plume Head		Ernst & Buchan 2002
Marked by transition in radiating dyke swarm from radiating to distal sub-linear pattern	B	Ernst et al. 1995
Marked by outer edge of flood basalt province (but lateral flow in dykes can emplace lavas and sills beyond plume edge)	B	White & McKenzie 1989; Ernst & Buchan 2002
Uplift causing interruption of sedimentation in pre-existing basins	B	Hill et al. 1992
OTHER POSSIBLE PLUME INDICATORS		
Sea-level changes Reflecting oceanic plateaus, but difficult to recognize against enhanced spreading, and supercontinent breakup	C	Kerr 1998; Eriksson 1999; Condie 2001
Iron formation (due to iron released from plumes)	B	Isley & Abbott 1999, Abbott & Isley 2001
Isotope record in marine carbonates		
Decrease in seawater $^{87}Sr/^{86}Sr$—enhanced oceanic plateau and spreading ridge volcanism	B	Kerr 1998, Wignall 2001
Decrease in seawater $^{18}O/^{16}O$—paleotemperature increase	C	Wignall 2001
Increase in seawater isotopic carbon: reflects carbon burial versus carbon recycling	C	Wignall 2001
Seawater $^{32}S/^{34}S$: reflects carbon cycling	C	Condie 2001
Extinction events	C	Wignall 2001, Courtillot et al. 1996
Meteorite impacts	D	Rampino & Stothers 1988, Isley & Abbott 2002, Jones et al. 2002
RECOGNITION OF "SUPERPLUME EVENTS"		
Plume clusters	B	Ernst & Buchan 2002
Association with geoid highs	B	Crough & Jurdy 1980, Pavonis 1997
Association with broad mantle upwellings underneath large plates	B	Davies 1999, Lowman & Gable 1999
Association with supercontinent breakup	B	e.g., Storey 1995, Li et al. 2003
Association with juvenile crust production (slab avalanche events)	C	Condie 2001
Association with lithospheric graveyards	C	Maruyama 1994, Fukao et al. 1994
Association with magnetic superchrons and periods of reduced reversal frequency	C	Johnson et al. 1995
Association with core resonance events	C	Greff-Lefftz & Legros 1999

The *Annual Review of Earth and Planetary Science* is online at http://earth.annualreviews.org

LITERATURE CITED

Abbott D, Isley A. 2001. Oceanic upwelling and mantle-plume activity: paleomagnetic tests of ideas on the source of the Fe in early Precambrian iron formations. See Ernst & Buchan 2001a, pp. 323–39

Abouchami W, Boher M, Michard A, Albarede F. 1990. A major 2.1 Ga event of mafic magmatism in West Africa: an early stage of crustal accretion. *J. Geophys. Res.* 95:17605–29

Agee CB. 1993. Petrology of the mantle transition zone. *Annu. Rev. Earth Planet. Sci.* 21:19–41

Albarède F, van der Hilst RD. 1999. New mantle convection model may reconcile conflicting evidence. *EOS Trans. Am. Geophys. Union* 80:535–39

Alvarez LW, Alvarez W, Asaro F, Michel HV. 1980. Extraterrestrial cause for the Cretaceous-Tertiary extinction: experimental results and theoretical interpretation. *Science* 208:1095–108

Anderson DL. 1995. Lithosphere, asthenosphere, and perisphere. *Rev. Geophys.* 33: 125–49

Arndt N. 1999. Why was flood volcanism on submerged continental platforms so common in the Precambrian? *Precambrian Res.* 97:155–64

Arndt N. 2000. Hot heads and cold tails. *Nature* 407:458–59

Arndt N, Bruzak G, Reischmann T. 2001. The oldest continental and oceanic plateaus: geochemistry of basalts and komatiites of the Pilbara craton, Australia. See Ernst & Buchan 2001a, pp. 359–87

Arndt N, Ginibre C, Chauvel C, Albarède F, Cheadle M, et al. 1998. Were komatiites wet? *Geology* 26:739–42

Arndt N, Weis D. 2002. Oceanic plateaus as windows to the Earth's interior: an ODP success story. *Joides J.* 28:79–84 (Spec. Issue)

Arndt NT. 1991. High Ni in Archean tholeiites. *Tectonophysics* 187:411–20

Arndt NT. 1994. Archean komatiites. In *Archean Crustal Evolution*, ed. KC Condie, pp. 11–44. Amsterdam: Elsevier

Ashwal LD. 1993. *Anorthosites.* New York: Springer-Verlag. 422 pp.

Ayer J, Amelin Y, Corfu F, Kamo S, Ketchum J, et al. 2002. Evolution of the southern Abitibi greenstone belt based on U-Pb geochronology: authochthonous volcanic construction followed by plutonism, regional deformation and sedimentation. *Precambrian Res.* 115:63–95

Bai W, Yang J-S, Fang Q-S, Shi R-D, Yan B-G. 2002. Unusual minerals in the podiform chromite of Luobusa, Tibet: do they come from lower mantle and how? In *Electronic Geosciences*, Vol. 7. *Extended Abstr. Photos Superplume Workshop, Tokyo.* http://link.springer.de/link/service/journals/10069/free/conferen/superplu/index.html

Bai WJ, Robinson PT, Fang Q-S, Yang J-S, Yan B-G, et al. 2000. The PGE and base-metal alloys in the podiform chromitites of the Luobusa ophiolite southern Tibet. *Can. Mineral.* 38:585–98

Bailey DK. 1993. Petrogenetic implications of the timing of alkaline, carbonatite, and kimberlite igneous activity in Africa. *S. Afr. J. Geol.* 96:67–74

Ballentine CJ, Lee D-C, Halliday AN. 1997. Hafnium isotopic studies of the Cameroon line and new HIMU paradoxes. *Chem. Geol.* 139:111–24

Baragar WRA. 1977. Volcanism of the stable crust. In *Volcanic Regimes in Canada*, ed. WRA Baragar, LC Coleman, JM Hall, *Geol. Assoc. Can. Spec. Pap.* 16:377–405

Baragar WRA, Ernst RE, Hulbert L, Peterson T. 1996. Longitudinal petrochemical variation in the Mackenzie dyke swarm,

northwestern Canadian Shield. *J. Petrol.* 37:317–59

Barbarin B. 1999. A review of the relationships between granitoid types, their origins and their geodynamic environments. *Lithos* 46:605–26

Barnes C, Hallam A, Kaljo D, Kauffman EG, Walliser OH. 1996. Global event stratigraphy. In *Global Events and Event Stratigraphy*, ed. OH Walliser, pp. 319–33. Berlin: Springer-Verlag

Barron EJ, Fawcett PJ, Peterson WH, Pollard D, Thompson SL. 1995. A "simulation" of Mid-Cretaceous climate. *Paleoceanography* 10:953–62

Basaltic Volcanism Study Project. 1981. *Basaltic Volcanism on the Terrestrial Planets.* New York: Pergamon. 1286 pp.

Basu AR, Poreda RJ, Renne PR, Teichmann F, Vasiliev YR, et al. 1995. High-^{3}He plume origin and temporal-spatial evolution of the Siberian flood basalts. *Science* 269:822–25

Bell K. 2001. Carbonatites: relationships to mantle-plume activity. See Ernst & Buchan 2001a, pp. 267–90

Bell K. 2002. Carbonatites and related alkaline rocks, lamprophyres, and kimberlites—indicators of mantle-plume activity. In *Electronic Geosciences*, Vol. 7. *Extended Abstr. Photos Superplume Workshop, Tokyo*. http://link.springer.de/link/service/journals/10069/free/conferen/superplu/index.html

Bell K, Tilton GR. 2001. Nd, Pb and Sr isotopic compositions of East African carbonatites: evidence for mantle mixing and plume inhomogeneity. *J. Petrol.* 42:1927–45

Bell K, Tilton GR. 2002. Probing the mantle: the story from carbonatites. *EOS Trans. Am. Geophys. Union* 83 (25):273–77

Bercovici D, Mahoney J. 1994. Double flood basalts and plume head separation at the 660-kilometer discontinuity. *Science* 266:1367–69

Bhushan SK. 2000. Malani rhyolites: a review. *Gondwana Res.* 3:65–77

Bizzarro M, Simonetti A, Stevenson RK, David J. 2002. Hf isotope evidence for a hidden mantle reservoir. *Geology* 30:771–74

Bleeker W, Parrish RR, Sager-Kinsman A. 1999. High-precision U-Pb geochronology of the Late Archean Kidd Creek deposit and Kidd Volcanic Complex. In *The Giant Kidd Creek Volcanogenic Massive Sulfide Deposit, Western Abitibi Subprovince, Canada*, ed. MD Hannington, CT Barrie, *Econ. Geol. Monogr.* 10:43–70

Bleeker W. 2002. Archaean tectonics: a review, with illustrations from the Slave craton. In *The Early Earth, Physical, Chemical and Biological Development. Geological Society Special Publication 199*, ed. CMR Fowler, CJ Ebinger, CJ Hawkesworth, pp. 151–81 London: Geol. Soc.

Blichert-Toft J, Boyet M, Télouk P, Albarède F. 2002. ^{147}Sm-^{143}Nd and ^{176}Lu-^{176}Hf in eucrites and the differentiation of the HED parent body. *Earth Planet. Sci.* 204:167–81

Brandon AD, Norman MD, Walker RJ, Morgan JW. 1999. ^{186}Os-^{187}Os systematics of Hawaiian picrites. *Earth Planet. Sci. Lett.* 174:25–42

Bryan SE, Riley TR, Jerram DA, Stephens CJ, Leat PT. 2002. Silicic volcanism: an undervalued component of large igneous provinces and volcanic rifted margins. See Menzies et al. 2002a, pp. 97–118

Buchan KL, Ernst RE, Hamilton MA, Mertanen S, Pesonen LJ, Elming S-A. 2001. Rodinia: the evidence from integrated palaeomagnetism and U-Pb geochronology. *Precambrian Res.* 110:9–32

Bultitude RJ. 1976. Flood basalts of probable early Cambrian age in northern Australia. In *Volcanism in Australasia: A Collection of Papers in Honour of the Late G.A.M. Taylor*, G.C., ed. RW Johnson, pp. 1–20. Amsterdam: Elsevier

Burke K. 1996. The African Plate. *S. Afr. J. Geol.* 99:341–409

Burke K. 1997. Foreward. In *Greenstone Belts*, ed. MJ de Wit, LD Ashwal, pp. v–vii. Oxford: Clarendon

Burke K, Dewey J. 1973. Plume-generated triple junctions: key indicators in applying plate tectonics to old rocks. *J. Geol.* 81:406–33

Caldeira K, Rampino MR. 1990. Deccan volcanism, greenhouse warming, and the Cretaceous/Tertiary boundary. *GSA Spec. Pap.* 247:117–23

Caldeira K, Rampino MR. 1991. The mid-Cretaceous superplume, carbon dioxide, and global warming. *Geophys. Res. Lett.* 18:987–90

Campbell IH. 1998. The mantle's chemical structure: insights from the melting products of mantle plumes. See Jackson 1998, pp. 259–310

Campbell IH. 2001. Identification of ancient mantle plumes. See Ernst & Buchan 2001a, pp. 5–21

Campbell IH. 2002. Implications of Nb/U, Th/U and Sm/Nd in plume magmas for the relationship between continental and oceanic crust formation and the development of the depleted mantle. *Geochim. Cosmochim. Acta* 66:1651–61

Campbell IH, Griffiths RW. 1990. Implications of mantle plume structure for the evolution of flood basalts. *Earth Planet. Sci. Lett.* 99:79–93

Campbell IH, Griffiths RW. 1992. The changing nature of mantle hotspots through time: implications for the geochemical evolution of the mantle. *J. Geol.* 92:497–523

Campbell IH, Griffiths RW. 1993. The evolution of the mantle's chemical structure. *Lithos* 30:389–99

Campbell IH, Hill RI. 1988. A two-stage model for the formation of the granite-greenstone terrains of the Kalgoorlie-Norseman area, Western Australia. *Earth Planet. Sci. Lett.* 90:11–25

Campbell IH, Griffiths RW, Hill RI. 1989. Melting in an Archaean mantle plume: heads it's basalts, tails it's komatiites. *Nature* 339:697–99

Chen YD, Liu SF. 1996. Precise U-Pb zircon dating of a post-D2 meta-dolerite: constraints for rapid tectonic development of the southern Adelaide Fold Belt during the Cambrian. *J. Geol. Soc. London* 153:83–90

Christiansen RL, Foulger GR, Evans JR. 2002. Upper-mantle origin of the Yellowstone hotspot. *GSA Bull.* 114:1245–56

Chumakov NM. 2001. General trend of climatic changes on the Earth during the last 3 Ga. *Doklady Acad. Nauk* 5:1034

Cloos M. 1993. Lithospheric buoyancy and collisional orogenesis: subduction of oceanic plateaus, continental margins, island arcs, spreading ridges and seamounts. *Geol. Soc. Am. Bull.* 105:715–37

Coffin MF, Eldholm O. 1994. Large igneous provinces: crustal structure, dimensions, and external consequences. *Rev. Geophys.* 32:1–36

Coffin MF, Eldholm O. 2001. Large igneous provinces: progenitors of some ophiolites? See Ernst & Buchan 2001a, pp. 59–70

Condie KC. 1997. Sources of Proterozoic mafic dyke swarms: constraints from Th/Ta and La/Yb ratios. *Precambrain Res.* 81:3–14

Condie KC. 2001. *Mantle Plumes and Their Record in Earth History*. Oxford, UK: Cambridge Univ. Press. 306 pp.

Condie KC. 2002. Continental growth during a 1.9-Ga superplume event. See Condie et al. 2002, 34:249–64

Condie KC, Abbott D, Des Marais DJ, eds. 2002. *Superplume Events in Earth History: Causes and Effects*. *Spec. Issue J. Geodyn.* 34:163–342

Cordery MC, Davies GF, Campbell IH. 1997. Genesis of flood basalts from eclogite-bearing mantle plumes. *J. Geophys. Res.* 102:20179–97

Courtillot V, Jaeger JJ, Yang Z, Féraud G, Hofmann C. 1996. The influence of continental flood basalts on mass extinctions: where do we stand? *GSA Spec. Pap.* 307:513–25

Courtillot V, Jaupart C, Manighetti I, Tapponnier P, Besse J. 1999. On causal links between flood basalts and continental breakup. *Earth Planet. Sci. Lett.* 166:177–95

Cox KG. 1989. The role of mantle plumes in the development of continental drainage patterns. *Nature* 342:873–77

Cox KG. 1993. Continental magmatic underplating. *Philos. Trans. R. Soc. London Ser. A* 342:155–66

Crough ST, Jurdy DM. 1980. Subducted lithosphere, hot spots, and the geoid. *Earth Planet. Sci. Lett.* 48:15–22

Czamanske GK, Gurevitch AB, Fedorenko V, Simonov O. 1998. Demise of the Siberian plume: paleogeographic and paleotectonic reconstruction from the prevolcanic and volcanic record, north-central Siberia. *Int. Geol. Rev.* 40:95–115

Davies GF. 1999. *Dynamic Earth: Plates, Plumes and Mantle Convection*. Oxford, UK: Cambridge Univ. Press. 458 pp.

Davis WJ. 1997. U-Pb zircon and rutile ages from granulite xenoliths in the Slave Province: evidence for mafic magmatism in the lower crust coincident with Proterozoic dike swarms. *Geology* 25:343–46

de Wit MJ. 1998. On Archean granites, greenstones, cratons and tectonics; does the evidence demand a verdict? *Precambrian Res.* 91:181–226

de Wit MJ, Ashwal LD. 1997. *Greenstone Belts.* Oxford Monogr. Geol. Geophys. Oxford, UK: Clarendon. 809 pp.

Dilek Y, Moores E, Elthon D, Nicolas A, eds. 2000. Ophiolites and oceanic crust: new insights from field studies and the ocean drilling program. *GSA Spec. Pap.* pp. 349, 552

Dobretsov NL, Vernikovsky VA. 2001. Mantle plumes and their geologic manifestations. *Int. Geol. Rev.* 43:771–87

Eales HV, Marsh JS, Cox KG. 1984. The Karoo igneous province: an introduction. *Geol. Soc. S. Afr. Spec. Publ.* 13:1–26

Earth Impact Database. 2002. http://www.unb.ca/passc/ImpactDatabase/ (Accessed: 15 June 2002)

Ebinger CJ, Sleep NH. 1998. Cenozoic magmatism throughout east Africa resulting from impact of a single plume. *Nature* 395:788–91

Eby GN. 1992. Chemical subdivision of the A-type granitoids: petrogenetic and tectonic implications. *Geology* 21:291–306

Eisele J, Sharma M, Galer SJG, Blichert-Toft J, Devey CW, Hofmann AW. 2002. The role of sediment recycling in EM-1 inferred from Os, Pb, Hf, Nd, Sr isotope and trace element systematics of the Pitcairn hotspot. *Earth Planet. Sci. Lett.* 196:197–212

Eriksson PG, Condie KC, van der Westhuizen W, van der Merwe R, de Bruiyn H, et al. 2002. Late Archaean superplume events: a Kaapvaal-Pilbara perspective. *J. Geodyn.* 34:207–47

Eriksson PG, Mazumder R, Sarkar S, Bose PK, Altermann W, van der Merwe R. 1999. The 2.7-2.0 Ga volcano-sedimentary record of Africa, India and Australia: evidence for global and local changes in sea level and continental freeboard. *Precambrian Res.* 97:269–302

Ernst RE, Baragar WRA. 1992. Evidence from magnetic fabric for the flow pattern of magma in the Mackenzie giant radiating dyke swarm. *Nature* 356:511–13

Ernst RE, Buchan KL. 1997a. Layered mafic intrusions: a model for their feeder systems and relationship with giant dyke swarms and mantle plume centres. *S. Afr. J. Geol.* 100:319–34

Ernst RE, Buchan KL. 1997b. Giant radiating dyke swarms: their use in identifying pre-Mesozoic large igneous provinces and mantle plumes. See Mahoney & Coffin 1997, pp. 297–333

Ernst RE, Buchan KL, eds. 2001a. *Mantle Plumes: Their Identification Through Time. GSA Am. Spec. Pap. 352.* 593 pp.

Ernst RE, Buchan KL. 2001b. Large mafic magmatic events through time and links to mantle plume heads. See Ernst & Buchan 2001a, pp. 483–575

Ernst RE, Buchan KL. 2001c. The use of mafic dike swarms in identifying and locating mantle plumes. See Ernst & Buchan 2001a, pp. 247–65

Ernst RE, Buchan KL. 2002. Maximum size and distribution in time and space of mantle plumes: evidence from large igneous provinces. See Condie et al. 2002, pp. 309–342 [Erratum, J. Geodyn. 34:711–14]

Fahrig WF. 1987. The tectonic settings of continental mafic dyke swarms: failed arm and early passive margin. In *Mafic Dyke Swarms,*

ed. HC Halls, WF Fahrig, pp. 331–48. *Geol. Assoc. Can. Spec. Pap. 34*

Fan J, Kerrich R. 1997. Geochemical characteristics of aluminum depleted and undepleted komatiites and HREE-enriched low-Ti tholeiites, western Abitibi greenstone belt: a heterogeneous mantle plume-convergent margin environment. *Geochim. Cosmochim. Acta* 61:4723–44

Farley KA, Natland JH, Craig H. 1992. Binary mixing of enriched and undegassed (primitive?) mantle components (He, Sr, Nd and Pb) in Samoan lavas. *Earth Planet. Sci. Lett.* 111:183–99

Förster H-J, Tischendorf G, Trumbull RB. 1997. An evaluation of the Rb vs. (Y + Nb) discrimination diagram to infer tectonic setting of silicic igneous rocks. *Lithos* 40:261–93

Forte AM, Mitrovica JX. 2001. Deep-mantle high-viscosity flow and thermochemical structure inferred from seismic and geodynamic data. *Nature* 410:1049–56

Fukao Y, Maruyama S, Obayashi M, Inoue H. 1994. Geologic implication of the whole mantle P-wave tomography. *J. Geol. Soc. Jpn.* 100:4–23 [pp. VI–VII (figure 16)]

Fukao Y, Widiyantoro S, Obayashi M. 2001. Stagnant slabs in the upper and lower mantle transition region. *Rev. Geophys.* 39:291–323

Gibson SA. 2002. Major element heterogeneity in Archean to Recent mantle plume startingheads. *Earth Planet. Sci. Lett.* 195:59–74

Goes S, Spakman W, Bijwaard H. 1999. A lower mantle source for central European volcanism. *Science* 286:1928–31

Gradstein FM, Ogg JG. 1996. A Phanerozoic time scale. *Episodes* 19:3–5

Granet M, Wilson M, Achauer U. 1995. Imaging a mantle plume beneath the French Massif Central. *Earth Planet. Sci. Lett.* 136:281–96

Greff-Lefftz M, Legros H. 1999. Core rotational dynamics and geological events. *Science* 286:1707–9

Grieve RAF, Shoemaker EM. 1994. The record of past impacts on Earth. In *Hazards Due to Asteroids and Comets*, ed. T Gehrel, pp. 417–62. Tucson: Univ. Ariz. Press

Griffin WL, Doyle BJ, Ryan CG, Pearson NJ, O'Reilly SY, et al. 1999. Layered mantle lithosphere in the Lac de Gras area, Slave craton: composition, structure, and origin. *J. Petrol.* 40:705–27

Griffiths RW, Campbell IH. 1990. Stirring and structure in mantle starting plumes. *Earth Planet. Sci. Lett.* 99:66–78

Griffiths RW, Campbell IH. 1991. Interaction of mantle plume heads with the Earth's surface and onset of small-scale convection. *J. Geophys. Res.* 96:18295–310

Grove TL, de Wit MJ, Dann J. 1997. Komatiites from the Komati type section. Barberton, South Africa. In *Greenstone Belts*, ed. MJ de Wit, LD Ashwal, pp. 422–37. Oxford, UK: Oxford Sci.

Haggerty SE. 1994. Superkimberlites: a geodynamic diamond window to the Earth's core. *Earth Planet. Sci. Lett.* 12:57–69

Haggerty SE. 1999a. Diamond formation and kimberlite-clan magmatism in cratonic settings. In *Mantle Petrology: Field Observation and High Pressure Experimentation: A Tribute to Francis R. (Joe) Boyd*, ed. Y-W Fei, CM Bertka, BO Mysen, pp. 105–23. Geochem. Soc. Spec. Publ. No. 6

Haggerty SE. 1999b. A diamond trilogy: superplumes, supercontinents, and supernovae. *Science* 285:851–60

Hames WE, McHone JG, Renne PR, Ruppel C, eds. 2003. *The Central Magmatic Province: Insights from Fragments of Pangea. AGU Geophys. Monogr. Ser.* 136:267

Hanan BB, Graham DW. 1996. Lead and helium isotope evidence from oceanic basalts for a common deep source of mantle plumes. *Science* 272:991–95

Hanley LM, Wingate MTD. 2000. SHRIMP zircon age for an Early Cambrian dolerite dyke: an intrusive phase of the Antrim Plateau volcanics of northern Australia. *Aust. J. Earth Sci.* 47:1029–40

Hansen U, Yuen DA. 2002. Superplumes as a critical threshold phenomenon. In *Electronic Geosciences*, Vol. 7. *Extended Abstr.*

Photos Superplume Workshop, Tokyo. http://link.springer.de/link/service/journals/10069/free/conferen/superplu/index.html.

Harland WB, Armstrong RL, Cox AV, Craig LE, Smith AG, Smith DG. 1990. *A Geological Time Scale 1989*. Cambridge: Cambridge Univ. Press. 263 pp.

Hart SR. 1988. Heterogeneous mantle domains: signatures, genesis and mixing chronologies. *Earth Planet. Sci. Lett.* 90:273–96

Hart SR, Hauri EH, Oschmann LA, Whitehead JA. 1992. Mantle plumes and entrainment: istopic evidence. *Science* 256:517–20

Hatton CJ, ed. 1997. Special issue on the proceedings of the Plumes, Plate and Mineralization '97 symposium. *S. Afr. J. Geol.* 100: 267–414

Hauri EH, Whitehead JA, Hart SR. 1994. Fluid dynamic and geochemical aspects of entrainment in mantle plumes. *J. Geophys. Res.* 99:24275–300

Heaman LM, Kjarsgaard BA. 2000. Timing of eastern North American kimberlite magmatism: Continental extension of the Great Meteor hotspot track? *Earth Planet. Sci. Lett.* 178:253–68

Helmstaedt HH. 1993. Primary diamond deposits. In *Giant Ore Deposits.*, ed. BH Whiting, R Mason, CJ Hodgson, *Soc. Econ. Geol. Spec. Publ.* 2:13–80

Herzberg C, O'Hara MJ. 1998. Phase equilibrium constraints on the origin of basalts, picrites, and komatiites. *Earth-Sci. Rev.* 44:39–79

Hildebrand AR, Penfield GT, Kring DA, Pilkington M, Camargo AZ, et al. 1991. Chicxulub Crater: a possible Cretaceous/Tertiary boundary impact crater on the Yucatan Peninsula, Mexico. *Geology* 19: 867–71

Hill RI. 1991. Starting plumes and continental break-up. *Earth Planet. Sci. Lett.* 104:398–416

Hill RI. 1993. Mantle plumes and continental tectonics. *Lithos* 30:193–206

Hill RI, Campbell IH, Davies GF, Griffiths RW. 1992. Mantle plumes and continental tectonics. *Science* 256:186–93

Hilton DR, Grönvold K, Macpherson CG, Castillo PR. 1999. Extreme $^{3}He/^{4}He$ ratios in northwest Iceland: constraining the common component in mantle plumes. *Earth Planet. Sci. Lett.* 173:53–60

Hirata T, Yang J-S. 2002. Re-Os and Hf-W isotopic systematics on Os and W metallic nuggests from Southern Tibet. In *Electronic Geosciences*, Vol. 7. *Extended Abstr. Photos Superplume Workshop, Tokyo*. http://link.springer.de/link/service/journals/10069/free/conferen/superplu/index.html.

Hofmann AW. 1997. Mantle geochemistry: the message from oceanic volcanism. *Nature* 385:219–29

Irvine GJ, Pearson DG, Kjarsgaard BA, Carlson RW, Kopylova MG, Dreibus G. 2003. Evolution of the lithospheric mantle beneath northern Canada: A Re-Os isotope and PGE study of kimberlite-derived peridotite xenoliths from Somerset Island and a comparison to the Slave and Kaapvaal cratons. *Lithos.* In press

Ishida M, Maruyama S, Suetsugu D, Matsuzaka S, Eguchi T. 1999. Superplume project: towards a new view of whole Earth dynamics. *Earth Planets Space* 51(1):i–v

Isley AE, Abbott DH. 2002. Implications of the temporal distribution of high-Mg magmas for mantle plume volcanism through time. *J. Geol.* 110:141–58

Isley AE, Abbott DH. 1999. Plume-related mafic volcanism and the deposition of banded iron formation. *J. Geophys. Res.* 104(B7):15461–77

J. Geol. Soc. Jpn. 1994. *J. Geol. Soc. Jpn.* 100:1–127

Jackson INS, ed. 1998. *The Earth's Mantle: Composition, Structure and Evolution.* New York: Cambridge Univ. Press. 566 pp.

Jahren AH. 2002. The biogeochemical consequences of the mid-Cretaceous superplume. See Condie et al. 2002, pp. 177–91

Johnson HP, Van Patten D, Tivey M, Sager WW. 1995. Geomagnetic polarity reversal rate for the Phanerozoic. *Geophys. Res. Lett.* 22:231–34

Jones AP, Price GD, Pricea NJ, DeCarli PS, Clegg RA. 2002. Impact induced melting and

the development of large igneous provinces. *Earth Planet. Sci. Lett.* 202:551–61

Kaminski E, Jaupart C. 2000. Lithosphere structure beneath the Phanerozoic intracratonic basins of North America. *Earth Planet. Sci. Lett.* 178:139–49

Keller GR, Bott MHP, Wendlandt RF, Doser DI, Morgan P. 1995. The Baikal rift system In *Continental Rifts: Evolution, Structure and Tectonics*, ed. KH Olsen, pp. 325–41. Amsterdam: Elsevier

Kellogg LH, Hager BH, van der Hilst RD. 1999. Compositional stratification in the deep mantle. *Science* 283:1881–84

Kelly A, Bercovici D. 1997. The clustering of rising diapirs and plume heads. *Geophys. Res. Lett.* 24:201–4

Kempton PD, Fitton JG, Saunders AD, Nowell GM, Taylor RN, et al. 2000. The Iceland plume in space and time: a Sr-Nd-Pb-Hf study of the North Altantic rifted margin. *Earth Planet. Sci. Lett.* 177:255–71

Kennett BLN, Van der Hilst RD. 1998. Seismic structure of the mantle: from subduction zone to craton. See Jackson 1998, pp. 381–404

Kennett BLN, Widiyantoro S. 1999. A low seismic wavespeed anomaly beneath northwestern India: a seismic signature of the Deccan plume? *Earth Planet. Sci. Lett.* 165:145–55

Kerr AC. 1994. Lithospheric thinning during the evolution of continental large igneous provinces. *Geology* 22:1027–30

Kerr AC. 1998. Oceanic plateau formation: a cause of mass extinction and black shale deposition around the Cenomanian-Turonian boundary. *J. Geol. Soc. London* 155:619–26

Kerr AC, Saunders AD, Tarney J, Berry NH, Hards VL. 1995. Depleted mantle-plume geochemical signatures: no paradox for plume theories. *Geology* 23:843–46

Kerr AC, Tarney J, Marriner GF, Nivia A, Saunders AD. 1997. The Caribbean-Colombian Cretaceous igneous province: the internal anatomy of an oceanic plateau. See Mahoney & Coffin 1997, pp. 123–44

Kerrich R, Wyman DA. 1997. Review of developments in trace-element fingerprinting of geodynamic settings and their implications for mineral exploration. *Austr. J. Earth Sci.* 44:465–87

Kerrich R, Xie Q. 2002. Compositional recycling structure of an Archean super-plume: Nb-Th-U-LREE systematics of Archean komatiites and basalts revisited. *Contrib. Mineral. Petrol.* 142:476–84

King SD, Anderson KL. 1998. Edge-driven convection. *Earth Planet. Sci. Lett.* 160:289–96

King PL, White AJR, Chappell BW, Allen CM. 1997. Characterization and origin of aluminous A-type granites from the Lachlan Fold Belt, southeastern Australia. *J. Pet.* 38:371–91

Klein GD. 1995. Intracratonic basins. In *Tectonics of Sedimentary Basins*, ed. CJ Busby, RV Ingersoll, pp. 459–78. Cambridge, MA: Blackwell Sci.

Klosko ER, Russo RM, Okal EA, Richardson WP. 2001. Evidence for a rheologically strong chemical mantle root beneath the Ontong-Java Plateau. *Earth Planet. Sci. Lett.* 186:347–61

Kumarapeli PS. 1993. A plume-generated segment of the rifted margin of Laurentia, southern Canadian Appalachians, seen through a completed Wilson Cycle. *Tectonophyiscs* 219:47–55

Larson RL. 1991a. Latest pulse of Earth: evidence for a mid-Cretaceous superplume. *Geology* 19:547–50

Larson RL. 1991b. Geological consequences of superplumes. *Geology* 19:963–66

Larson RL. 1997. Superplumes and ridge interactions between Ontong Java and Manihiki Plateaus and the Nova-Canton Trough. *Geology* 25:779–82

Larson RL, Olson P. 1991. Mantle plumes control magnetic reversal frequency. *Earth Planet. Sci. Lett.* 107: 437–47

Lassiter JC, DePaolo DJ. 1997. Plume/lithosphere interaction in the generation of continental and oceanic flood basalts: chemical and isotopic constraints. See Mahoney & Coffin 1997, pp. 335–55

Le Bas MJ. 2000. IUGS reclassification of the

high-Mg and picritic rocks. *J. Pet.* 41:1467–70

Leitch AM, Davies GD. 2001. Mantle plumes and flood basalts: enhanced melting from plume ascent and an eclogite component. *J. Geophys. Res.* 106:2047–59

Li ZX, Li XH, Kinny PD, Wang J. 1999. The breakup of Rodinia: Did it start with a mantle plume beneath South China? *Earth Planet. Sci. Lett.* 173:171–81

Li ZX, Li XH, Kinny PD, Wang J, Zhang S, Zhou H. 2003. Geochronology of Neoproterozoic syn-rift magmatism in the Yangtze Craton, South China and correlations with other continents: evidence for a mantle superplume that broke up Rodinia. *Precambrian Res.* In press

Lithgow-Bertelloni C, Silver PG. 1998. Dynamic topography, plate driving forces, and the African superswell. *Nature* 395: 269–72

Loper DE, McCartney K. 1990. On impacts as a cause of geomagnetic field reversals or flood basalts. In *Global Catastrophes in Earth History: An Interdisciplinary Conference on Impacts, Volcanism, and Mass Mortality. GSA Spec. Pap. 247*, ed. VL Sharpton, PD Ward, pp. 19–25. Colorado: Geol. Soc. Am.

Lowman JP, Gable CW. 1999. Thermal evolution of the mantle following continental aggregation in 3D convection models. *Geophys. Res. Lett.* 26:2649–52

Ludden JN, Arndt NT, Francis D, eds. 1996. Mafic magmatism through time. *Lithos* (Spec. Issue) 37:79–280

Maclennan J, Lovell B. 2002. Control of regional sea level by surface uplift and subsidence caused by magmatic underplating of Earth's crust. *Geology* 30:675–78

Mahoney J, Coffin M, eds. 1997. *Large Igneous Provinces: Continental, Oceanic, and Planetary Volcanism, AGU Geophys. Monogr. Ser.* 100:438

Maruyama S. 1994. Plume tectonics. *J. Geol. Soc. Jpn.* 100:24–49

McGhee GR Jr. 2001. The 'multiple impacts hypothesis' for mass extinction: a comparison of the Late Devonian and the late Eocene. *Palaeogeogr. Palaeoclimatol. Palaeoecol.* 176:47–58

McNutt MK. 1998. Superswells. *Rev. Geophys.* 36:211–44

Mège D. 2001. Uniformitarian plume tectonics: the post-Archean Earth and Mars. See Ernst & Buchan 2001a, pp. 141–64

Mège D, Ernst RE. 2001. Contractional effects of mantle plumes on Earth, Mars and Venus. See Ernst & Buchan 2001a, pp. 103–40

Melosh HJ. 2001. Impact-induced volcanism: a geologic myth. *Abstr. Progr.* 33 (No. 6):A433. GSA Annu. Meet., Boston

Menzies MA, Klemperer SL, Ebinger CJ, Baker J, eds. 2002a. Volcanic *Rifted Margins GSA Spec. Pap.* 362. 230 pp.

Menzies MA, Klemperer SL, Ebinger CJ, Baker J. 2002b. Characteristics of volcanic rifted margins. See Menzies et al. 2002a, pp. 1–14

Meschede M. 1986. A method of discriminating between different types of mid-ocean ridge basalts and continental tholeiites with the Nb-Zr-Y diagram. *Chem. Geol.* 56:207–18

Mitchell RH. 1995. *Kimberlites, Orangeites, and Related Rocks.* New York: Plenum Press. 410 pp.

Monnereau M, Rabinowicz M, Arquis E. 1993. Mechanical erosion and reheating of the lithosphere: a numerical model for hotspot swells. *J. Geophys. Res.* 98:809–23

Moores EM. 2002. Ophiolites and plumes in Earth history, their tectonic and environmental implications. In *Electronic Geosciences*, Vol. 7. *Extended Abstr. Photos Superplume Workshop, Tokyo.* http://link.springer.de/link/service/journals/10069/free/conferen/superplu/index.html

Morgan WJ. 1971. Convection plumes in the lower mantle. *Nature* 230:42–43

Morgan WJ. 1972. Plate motions and deep mantle convection. In *Studies in Earth and Space Sciences. GSA Mem.* 132, ed. R Shagam, RB Hargraves, WJ Morgan, FB Van Houten, CA Burk, et al. pp. 7–22. New York: Geol. Soc. Am.

Moser DE, Heaman LM. 1997. Proterozoic zircon growth in Archean lower crustal xenoliths, southern Superior craton—a

consequence of Matachewn ocean opening: *Contrib. Mineral. Petrol.* 128:164–75

Murphy JB, Oppliger GL, Brimhall GH Jr, Hynes A. 1998. Plume-modified orogeny: an example from the western United States. *Geology* 26: 731–34

Nataf H-C. 2000. Seismic imaging of mantle plumes. *Annu. Rev. Earth Planet. Sci.* 28:391–417

Neal CR, Mahoney JJ, Kroenke LW, Duncan RA, Petterson MG. 1997. The Ontong Java plateau. See Mahoney & Coffin 1997, pp. 183–216

Nowell GM, Kempton PD, Noble SR, Fitton JG, Saunders AD, et al. 1998. High precision Hf isotope measurements of MORB and OIB by thermal ionisation mass spetrometry: insights into the depleted mantle. *Chem. Geol.* 149:211–33

Niu F, Solomon SC, Silver PG, Suetsugu D, Inoue H. 2002. Mantle transition-zone structure beneath the South Pacific Superswell and evidence for a mantle plume underlying the Society hotspot. *Earth Planet. Sci. Lett.* 198:371–80

Okulitch AV. 2002. Geological time chart, 2002. *Geol. Surv. Can., Open File 3040.* (Natl. Earth Sci. Ser., Geol. Atlas) Revis.

Olsen PE, Kent DV, Sues H-D, Koeberl C, Huber H, et al. 2002. Ascent of dinosaurs linked to an iridium anomaly at the Triassic-Jurassic boundary. *Science* 296:1305–7

O'Nions RK, Tolstikhin IN. 1996. Limits on the mass flux between lower and upper mantle and stability of layering. *Earth Planet. Sci. Lett.*. 139:213–22

Orovetskii YuP. 1999. *Mantle Plumes*. Rotterdam, The Netherlands: Balkema. 245 pp.

Pálfy J, Parrish RR, Smith PL. 1997. A U-Pb age from the Toarcian (Lower Jurassic) and its use for time scale calibration through error analysis of biochronologic dating. *Earth Planet. Sci. Lett.* 146:659–75

Pálfy J, Smith PL. 2000. Synchrony between Early Jurassic extinction, oceanic anoxic event, and the Karoo-Ferrar flood basalt volcanism. *Geology* 28:747–50

Pálfy J, Smith PL, Mortensen JK. 2000. A U-Pb and ^{40}Ar-^{39}Ar time scale for the Jurassic. *Can. J. Earth Sci.* 37:923–44

Pankhurst RJ, Leat PT, Sruoga P, Rapela CW, Márquez M, et al. 1998. The Chon Aike province of Patagonia and related rocks in West Antarctica: a silicic large igneous province. *J. Volcanol. Geotherm. Res.* 81:113–36

Parsons T, Thompson GA, Smith RP. 1998. More than one way to stretch: a tectonic model for extension along the plume track of the Yellowstone hotspot and adjacent Basin and Range province. *Tectonics* 17:221–34

Passchier CW. 1995. Precambrian orogenesis: was it really different? *Geol. Mijnb.* 74:141–50

Pavoni N. 1997. Geotectonic bipolarity-evidence of bicellular convection on the Earth's mantle. *S. Afr. J. Geol.* 100:291–99

Pearce JA, Cann JR. 1973. Tectonic setting of basic volcanic rocks determined using trace element analyses. *Earth Planet. Sci. Lett.* 19:290–300

Pearce JA, Harris NWB, Tindle AG. 1984. Trace element determination diagrams for the tectonic interpretation of granitic rocks. *J. Pet.* 25:956–83

Pearson DG. 1999. The age of continental roots. *Lithos* 48:171–94

Peucker-Ehrenbrink B, Ravizza G. 2000. The marine osmium isotope record. *Terra Nova* 12:205–19

Pirajno F. 2000. *Ore Deposits and Mantle Plumes*. Dordrecht, Neth: Kluwer Acad. 556 pp.

Poag CW. 1997. The Chesapeake Bay bolide impact: a convulsive event in Atlantic Coastal plain evolution. *Sediment. Geol.* 108:45–90

Prokoph A, Veizer J. 1999. Trends, cycles and nonstationarities in isotope signals of Phanerozoic seawater. *Chem. Geol.* 161:225–40

Rainbird R, Ernst RE. 2001. The sedimentary record of mantle-plume uplift. See Ernst & Buchan 2001a, pp. 227–45

Rampino MR, Stothers RB. 1988. Flood basalt volcanism during the past 250 million years. *Science* 241:663–68

Reichow MK, Saunders AD, White RV, Pringle MS, Al-Mukhamedov AI, Medvedev AI, Kirda NP. 2002. $^{40}Ar/^{39}Ar$ dates from the West Siberian basin: Siberian flood basalt province doubled. *Science* 296:1846–49

Richardson WP, Okal EA, VanderLee S. 2000, Rayleigh-wave tomography of the Ontong-Java Plateau. *Phys. Earth Planet. Inter.* 118:29–51

Sasada T, Hiyagon H, Bell K, Ebihara M. 1997. Mantle-derived noble gases in carbonatites. *Geochim. Cosmochim. Acta* 61:4219–28

Saunders AD, Fitton JG, Kerr AC, Norry MJ, Kent RW. 1997. The North Atlantic Igneous Province. See Mahoney & Coffin 1997, pp. 45–93

Schissel D, Smail R. 2001. Deep-mantle plumes and ore deposits. See Ernst & Buchan 2001a, pp. 291–322

Schubert G, Turcotte DL, Olson P. 2001. *Mantle convection in the Earth and Planets*. Cambridge Univ. Press. 940 pp.

Şengör AMC. 1995. Sedimentation and tectonics of fossil rifts. In *Tectonics of Sedimentary Basins*, ed. CJ Busby, RV Ingersoll, pp. 53–117. Cambridge, MA: Blackwell Sci.

Şengör AMC. 2001. Elevation as indicator of mantle-plume activity. See Ernst & Buchan 2001a, pp. 183–225

Şengör AMC, Natal'in BA. 2001. Rifts of the world. See Ernst & Buchan 2001a, pp. 389–482

Sheehan PM. 2001. The Late Ordovician mass extinction. *Annu. Rev. Earth Planet. Sci.* 29:331–64

Shen Y, Soloman SC, Bjarnason IT, Nolet G, Morgan WJ, et al. 2002. Seismic evidence for a tilted mantle plume and north-south mantle flow beneath Iceland. *Earth Planet. Sci. Lett.* 197:261–72

Shervais JW. 1982. Ti-V plots and the petrogenesis of modern and ophiolitic lavas. *Earth Planet. Sci. Lett.* 59:101–18

Shirey SB, Walker RJ. 1998. The Re-Os isotope system in cosmochemistry and high-temperature geochemistry. *Annu. Rev. Earth Planet. Sci.* 26:423–500

Sleep NH. 1990. Hotspots and mantle plumes: some phenomenology. *J. Geophys. Res.* 95: 6715–36

Smith AD, Lewis C. 1999. The planet beyond the plume hypothesis. *Earth-Sci. Rev.* 48:135–82

Solomon SC, Bullock MA, Grinspoon DH. 1999. Climate change as a regulator of tectonics on Venus. *Science* 286:87–90

Sproule RA, Lesher CM, Ayer JA, Thurston PC, Herzberg CT. 2002. Spatial and temporal variations in the geochemistry of komatiites and komatiitic basalts in the Abitibi greenstone belt. *Precambrian Res.* 115:153–86

Stein M, Hofmann AW. 1992. Fossil plume head beneath the Arabian lithosphere? *Earth Planet. Sci. Lett.* 114: 193–209

Storey BC. 1995. The role of mantle plumes in continental breakup: case histories from Gondwanaland. *Nature* 377:301–8

Storey BC, Kyle PR. 1997. An active mantle mechanism for Gondwana breakup. *S. Afr. J. Geol.* 100:283–90

Tackley PJ, Stevenson DJ, Glatzmaier GA, Schubert G. 1993. Effects of an endothermic phase transition at 670 km depth in a spherical model of convection in the Earth's mantle. *Nature* 361:699–704

Takahashi E, Nakajima K, Wright TL. 1998. Origin of the Columbia River basalts: melting model of a heterogeneous plume head. *Earth Planet. Sci. Lett.* 162:63–80

Tan E, Gurnis M, Han L. 2002. Slabs in the lower mantle and their modulation of plume formation. *Geochem. Geophys. Geosyst.* 3(11):1067 doi:10.1029/2001/GC000238

Thompson RN, Gibson SA. 1991. Subcontinental mantle plumes, hotspots and pre-existing thinspots. *J. Geol. Soc. London* 148:973–77

Thompson RN, Morrison MA, Dickin AP, Hendry GL. 1983. Continental flood basalts . . . arachnids rule OK? *Continental Basalts and Mantle Xenoliths*, ed. CJ Hawkesworth, MJ Norry, pp. 158–85. Cheshire UK: Shiva Publishing Ltd.

Thurston PC, Chivers KM. 1990. Secular variation in greenstone sequence development emphasizing Superior Province, Canada. *Precambrian Res.* 46:21–58

Tomlinson KY, Condie KC. 2001. Archean mantle plumes: evidence from greenstone belt geochemistry. See Ernst & Buchan 2001a, pp. 341–57

Torsvik TH, Carter LM, Ashwal LD, Bhushan SK, Pandit MK, Jamtveit B. 2001. Rodinia refined or obscured: palaeomagnetism of the Malani igneous suite (NW India). *Precambrian Res.* 108: 319–33

VanDecar JC, James DE, Assumpção M. 1995. Seismic evidence for a fossil mantle plume beneath South America and implications for plate driving forces. *Nature* 378:25–31

van der Hilst RD, Widiyantoro S, Engdahl ER. 1997. Evidence for deep mantle circulation from global tomography. *Nature* 386:578–84

van Keken PE, Hauri EH, Ballentine CJ. 2002. Mantle mixing: the generation, preservation, and destruction of chemical heterogeneity. *Annu. Rev. Earth Planet. Sci.* 30:493–525

Veizer J, Ala D, Azmy K, Bruckschen P, Buhl D, et al. 1999. $^{87}Sr/^{86}Sr$, $\delta^{13}C$ and $\delta^{18}O$ evolution of Phanerozoic seawater. *Chem. Geol.* 161:59–88

Walker RJ. 2002. Tracing the osmium isotopic compositions of large plumes through Earth history. In *Electronic Geosciences*, Vol. 7. *Extended Abstr. Photos Superplume Workshop, Tokyo.* http://link.springer.de/link/service/journals/10069/free/conferen/superplu/index.html

Whalen JB, Currie KL, Chappell BW. 1987. A-type granites: geochemical characteristics, discrimination and petrogenesis. *Contrib. Mineral. Petrol.* 95:407–19

White N, Lovell B. 1997. Measuring the pulse of a plume with the sedimentary record. *Nature* 387:888–91

White RS, McKenzie D. 1989. Magmatism at rift zones: the generation of volcanic continental margins and flood basalts. *J. Geophys. Res.* 94:7685–29

White RS, McKenzie D. 1995. Mantle plumes and flood basalts. *J. Geophys. Res.* 100:17543–85

Wignall PB. 2001. Large igneous provinces and mass extinctions. *Earth-Sci. Rev.* 53:1–33

Williams GE. 1994. Resonances of the fluid core for a tidally decelerating Earth: cause of increased plume activity and tectonothemal reworking events? *Earth Planet. Sci. Lett.* 128:155–67

Williams GE, Gostin VA. 2000. Mantle plume uplift in the sedimentary record: origin of kilometre-deep canyons within late Neoproterozoic successions, South Australia. *J. Geol. Soc. London* 157:759–68

Wilson JT. 1963. A possible origin of the Hawaiian Islands. *Can. J. Earth Sci.* 41:863–70

Wilson L, Head JW. 2002. Tharsis-radial graben systems as the surface manifestation of plume-related dike intrusion complexes: models and implications. *J. Geophys. Res.* 107 (E8): 1-1-1-24, DOI 10.1029/2001JE001593

Wilson M. 1997. Thermal evolution of the Central Atlantic passive margins: continental break-up above a Mesozoic super-plume. *J. Geol. Soc. London* 154:491–95

Wilson M, Patterson R. 2001. Intraplate magmatism related to short-wavelength convective instabilities in the upper mantle: Evidence from the Tertiary-Quaternary volcanic province of western and central Europe. See Ernst & Buchan 2001a, pp. 37–58

Winchester JA, Floyd PA. 1977. Geochemical discrimination of different magma series and their differentiation products using immobile elements. *Chem. Geol.* 20:325–43

Windley BF, Maruyama S. 2002. Where was the birth site of the Pacific and African superplumes? In *Electronic Geosciences*, Vol. 7. *Extended Abstr. Superplume Workshop, Tokyo.* http://link.springer.de/link/service/journals/10069/free/conferen/superplu/index.html

Woolley AR. 1989. The spatial and temporal distribution of carbonatites. In *Carbonatites: Genesis and Evolution*, ed. K Bell, pp. 15–37. London: Unwin Hyman

Worsley TR, Nance RD, Moody JB. 1986. Tectonic cycles and the history of the Earth's biogeochemical and paleoceanographic record. *Paleoceanography* 1:233–63

Wyman DA. 1999. A 2.7 Ga depleted tholeiite suite: evidence of plume-arc interation in the Abitibi belt, Canada. *Precambrian Res.* 97:27–42

Wyman DA, Bleeker W, Kerrich R. 1999. A 2.7 Ga komatiite, low Ti tholeiite, arc tholeiite transition, and inferred proto-arc geodynamic setting of the Kidd Creek deposit: evidence from precise trace element data. In *The Giant Kidd Creek Volcanogenic Massive Sulfide Deposit, Western Abitibi Subprovince, Canada*, ed. MD Hannington, CT Barrie, *Econ. Geol. Monogr.* 10:511–28

Wyman DA, Kerrich R. 2002. Formation of Archean continental lithospheric roots: the role of mantle plumes. *Geology* 30:543–46

Xie Q, Kerrich R. 1994. Silicate-perovskite and majorite signature komatiites from Archean Abitibi Belt: implications for early mantle differentiation and stratification. *J. Geophys. Res.* 99: 15799–812

Xie Q, Kerrich R, Fan J. 1993. HFSE/REE fractionations recorded in three komatiite-basalt sequences, Archean Abitibi greenstone belt: implications for multiple plume sources and depths. *Geochim. Cosmochim. Acta* 57:4111–18

Zhao D. 2001. Seismic structure and origin of hotspots and mantle plumes. *Earth Planet. Sci. Lett.* 192:251–65

Zindler A, Hart SR. 1986. Chemical geodynamics. *Annu. Rev. Earth Planet. Sci* 14:493–571